BEH YONG HUAT B. ENG (HONS) MECHANICAL ENGINEERING JANUARY 2016

MEASUREMENT OF WATER IN OIL PIPELINES USING CAPACITANCE METHOD

BEH YONG HUAT

MECHANICAL ENGINEERING
UNIVERSITI TEKNOLOGI PETRONAS
JANUARY 2016

Measurement of Water in Oil Pipelines

using Capacitance Method

by

Beh Yong Huat
16266

Dissertation submitted in partial fulfilment of
the requirements for the
Bachelor of Engineering (Hons)
Mechanical Engineering

JANUARY 2016

Universiti Teknologi PETRONAS
Bandar Seri Iskandar
31750 Tronoh
Perak Darul Ridzuan

CERTIFICATION OF APPROVAL

Measurement of Water in Oil Pipelines
using Capacitance Method

by

Beh Yong Huat
16266

A project dissertation submitted to the
Mechanical Engineering Programme
Universiti Teknologi PETRONAS
in partial fulfillment of the requirement for the
BACHELOR OF ENGINEERING (Hons)
MECHANICAL ENGINEERING

Approved by,

_____

(Dr. William Pao King Soon)

UNIVERSITI TEKNOLOGI PETRONAS
TRONOH, PERAK
January 2016

CERTIFICATION OF ORIGINALITY

This is to certify that I am responsible for the work submitted in this project, that the original work is my own except as specified in the references and acknowledgements, and that the original work contained herein have not been undertaken or done by unspecified sources or persons.

_____

BEH YONG HUAT

ABSTRACT

This project entitled “Measurement of Water in Oil Pipelines using Capacitance Method” is closely related to oil & gas industry especially from the aspect of safety. To minimize the internal corrosion of oil pipelines due to the presence of water, capacitance method is introduced to detect the amount of water present in oil-water mixture. Being cheap, safe and non- intrusive, this method is suitable for two-phase fluids with low conductivity and large permittivity difference such as oil and water. However, different configurations of electrodes will produce different results in terms of linearity of response. In this project, by utilising ANSYS Maxwell software, two common configurations of electrodes i.e. concave and double rings electrodes are designed to compare their linearity of response towards changes in water content in oil-water mixture. Simulation is performed where double rings electrode is more superior to concave electrode in terms of linearity of response. Besides that, sensitivity analysis is carried out on concave electrodes. Both two-plate and four-plate sensors are investigated and compared in terms of the average sensitivity and sensitivity variation parameters. The average sensitivity of sensors is greatly increased during the shift from two-plate design to four-plate design. However, this causes the sensitivity variation parameter to be increased as well. 40° electrode angle is found out to be the optimum four-plate concave electrodes based on the higher average sensitivity of 2.8141 and lower sensitivity variation parameter of 0.29 % as compared to 80° electrode angle of two-plate design. As the recommendation, experimental works can be carried out in future to validate the simulation results obtained.

ACKNOWLEDGEMENT

My completion of Final Year Project will not be a success without the support from many people directly or indirectly involved. Hereby, I would like to acknowledge my upmost gratitude to those people I honor.

First of all, I would like to take this opportunity to express my profound gratitude and deep regards to my supervisor, Dr. William Pao King Soon, for his exemplary guidance, monitoring and constant encouragement throughout this thesis. His insights on several technical aspects have been really helpful in assisting my work. Besides that, from his sharing of experience in life, I gain a lot of values which are useful for my self-development in both current study and future working environment.

Next, I would also like to express my gratitude to a master's student, Mr. Lim Lam Ghai, who are currently doing a related research in UTP. Through several fruitful discussions with him, it helps me to improve my knowledge and skills required in this project immensely. In addition, I would also like to thank all my colleagues in giving their comments and suggestions for my work. Last but not least, I would like to thank almighty and my beloved family members for their support throughout the eight months of my Final Year Project.

TABLE OF CONTENT

LIST OF FIGURES

LIST OF TABLES

CHAPTER 1
INTRODUCTION

1.1 Project background

Figure 1.1: Internally corroded oil pipeline [1]

The aspect of Health, Safety and Environment (HSE) has always been top priority in petroleum industry for reputation and integrity of oil & gas companies [2]. The long distance transmission of oil using pipelines from offshore platform to refinery plant is a big challenge as it faces the risk of internal corrosion, as illustrated in Figure 1.1 above, which can lead to rupture and oil leakage. The presence of water, a type of defect, cannot be easily detected [3]. To avoid huge amount of money spent on replacing the corroded pipelines, water has to be detected and removed to prevent corrosion. Inspection on crude oil with the measurement of water content is essential to make sure that it is constantly under the safety level of 0.5% for the ideal case [4].

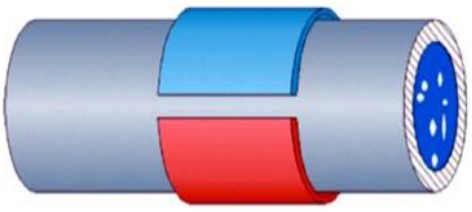

Figure 1.2: Capacitive sensors on pipe wall [5]

Here, capacitance method will be introduced as a suitable water detection technique which is cheap, simple and non-intrusive. It has an obvious advantage where the large difference in dielectric constant for oil and water allows accurate measurement of water content in oil-water mixture [6]. As shown in Figure 1.2 above, this method involves the application of two capacitive sensors mounted around the pipe wall. In this project, the performance of different configurations of electrodes as well as the resolution of water detection will be investigated.

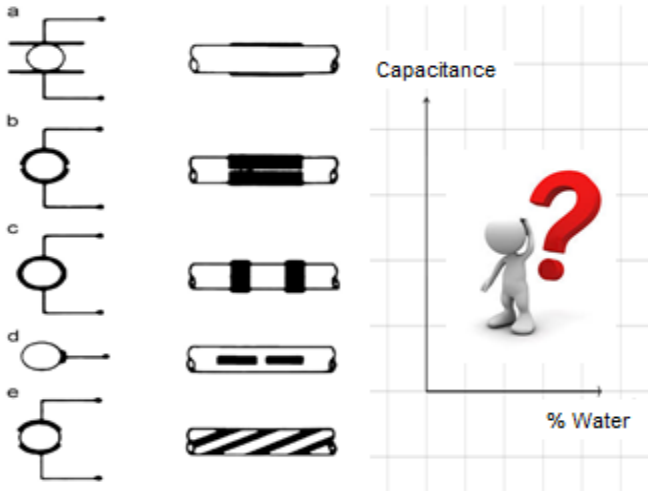

Figure 1.3: Dependency of results on electrodes configurations [5]

1.2 Problem statement

The core problem faced in this research paper is the presence of water in oil pipelines. As one of the elements required for corrosion, moisture will certainly speed up the internal corrosion rate of the pipe wall in a daily basis [7]. To date, various conventional techniques have been applied in measurement of water composition but all are having their own limitations in terms of cost, safety, complexity and intrusive nature, making them unfavorable to be adopted. Meanwhile results obtained from these methods are generally low in linearity and sensitivity.

For the implementation of capacitance method as proposed in this project, the primary factor affecting the result is the configuration of electrodes namely helical, concave and double ring electrodes in general to be mounted on the pipe wall [8]. The main problem

raised is that all configurations perform differently in terms of linearity of response during the phase volume fraction measurement of oil-water mixture. Also, specifically for concave electrodes, the current two-plate capacitance sensors have low homogeneity of sensitivity, highlighting the issue of dependency of the capacitance measurement on the location of equal-volume elements throughout the fluid.

1.3 Objectives

In this project, the objectives have been identified and listed down as follow:

i. To prove the capacitance method as a feasible measurement technique for the detection of water in oil pipelines.
ii. To compare concave electrodes and double rings electrodes in terms of linearity of response with varying water content in oil-water mixture.
i. To perform sensitivity analysis on concave electrodes and compare the results for two-plate and four-plate capacitance sensors.

1.4 Scope of study

In this project, the transportation of oil in oil & gas industry facing the issue of corrosion due to the presence of water will be explored. Next, capacitance method will be introduced as a feasible water fraction measurement method where its advantages and basic operating principle will be covered. Also, the common configurations of electrodes in this method will be discussed and compared.

Besides that, knowledge on two-phase flow is required in this project where the fluids involved are oil and distilled water. This project includes the volume fraction measurement technique in capacitance method where ANSYS Maxwell software will be utilized for the simulation of oil-water mixture using double rings electrodes and concave electrodes. Sensitivity analysis will be carried out as well to compare the performance of double rings and concave capacitance. Parameters such as sensor relative sensitivity and sensitivity variation parameter will be explored as the basis of comparison. In this project, there will be no experimental works carried out.

CHAPTER 2
LITERATURE REVIEW

2.1 Oil pipelines and capacitance method

In oil and gas industry, in most cases, the oil extracted will be mixed with water in the oil transmission pipelines between the offshore platform and refinery terminal in the mainland. This is due to ineffective oil extraction or treatment process to remove impurities, i.e. water at the platform after drilling [3]. According to Biomogi et al, the typical amount of water found in crude oil is around 1.5% [3]. The presence of water is considered as a type of defects since it can lead to internal corrosion of pipes.

Internal corrosion will result in loss of pipe wall metal where the pipe wall thickness will reduce slowly before rupture might occur due to high pressure, leading to huge economic losses [2]. Also, if hydrocarbon is mixed with water, the tendency of corrosion increases due to the reduction in pH value. For example of an iron pipe, the presence of water will encourage corrosion as a result of oxidation and reduction at the pipe and water respectively as described by Eq. (2.1) and Eq. (2.2) below, respectively [2]:

$$Fe \xrightarrow{oxidation} Fe^{2+} + 2e^{-} \tag{2.1}$$

$$2H_2O + O_2 + 4e^{-} \xrightarrow{reduction} 4OH^{-} \tag{2.2}$$

One of the most famous incidents is Prudhoe Bay oil spill in Alaska in 2006.

For the sake of integrity, oil and gas companies have spent billions of money each year to keep their pipelines safe from any internal corrosion through application of corrosion inhibitors and etc. [7]. Statistic [2] illustrates that corrosion is the second largest factor of crude oil pipelines failure in USA as shown in Figure 2.1 below, addressing the seriousness of this issue and the need to formulate a solution.

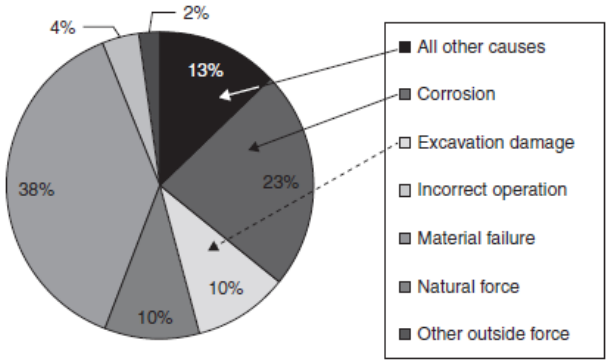

Figure 2.1: Factors of pipelines failure in USA [2]

In oil and gas industry, the presence of moisture in oil is often undesirable and a lot of techniques have been introduced by previous researchers in their study to carry out a proper volume fraction measurement [9]. Table 2.1 below summarizes those methods with related details for comparison. Of all methods mentioned, capacitance method is selected to be the most suitable technique to be adopted for study on oil water flow.

Table 2.1: Summary of volume fraction measurement methods [9-18]

Authors	Methods	Results	Limitations
Ebbe and Arnstein, Yu et al. and Wylie et al. [9-11]	Microwave and Radio Frequency	High error	Complex circuit design
Lakar and Bordoloi [12]	Optical	Low linearity	Liquids and wall must be transparent
Martijn et al. [13,14]	X-ray and Gamma ray	Around 2 -3 % error	Complex, expensive and health risk
Mohd et al. [15]	Ultrasonic	Low linearity	Superposition of signals
Silva et al. [16]	Wire-mesh	625 frames/s	Intrusive
Tsochatzidis et al. [17]	Conductance	Low sensitivity	Intrusive
Domenico et al. [18]	Capacitance	Linearity and high sensitivity	Electrical losses for conductive fluids

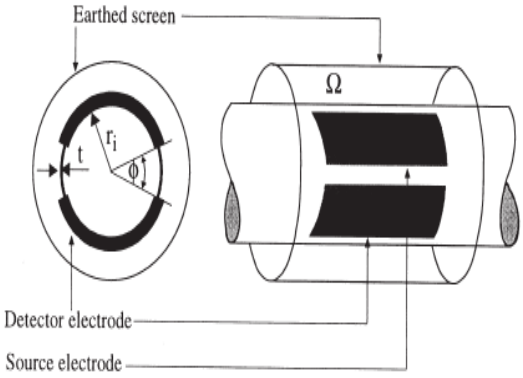

Figure 2.2: Typical setup of capacitance method [19]

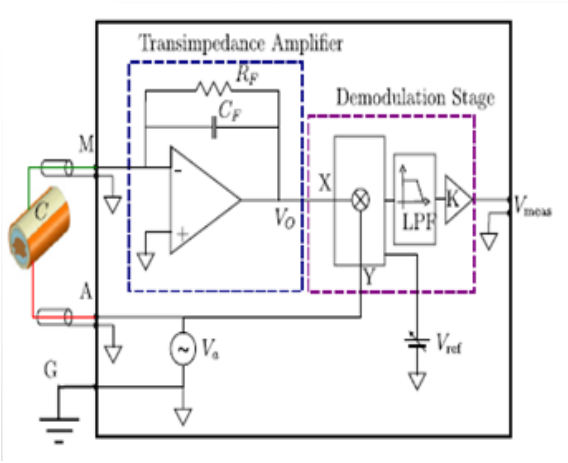

Figure 2.3: Equivalent block diagram [18]

The typical setup of capacitance method for water detection in a pipe is illustrated in Figure 2.2 above. Basically it involves two electrodes as the sensors. This method can be represented by a block diagram that contains its basic operating principle, starting from the attachment to the pipe to the measurement of voltage values, as shown in Figure 2.3. Compared to other conventional methods, capacitance method is able to produce results of high sensitivity and linearity besides having low possibility of error. Also, its advantages include low complexity, low cost, non-intrusive and safe [18]. The safety aspect of capacitance method is the key for its further development in near future.

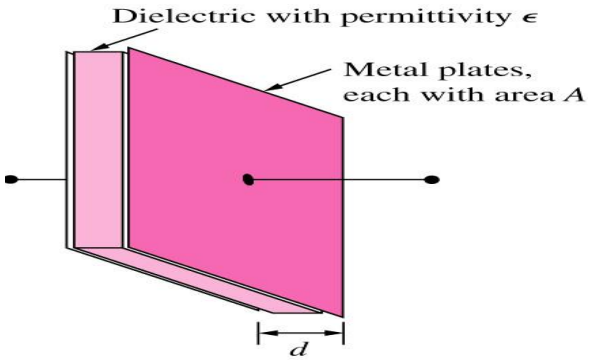

Figure 2.4: Parallel-plate capacitor [20]

Capacitance is defined as the ability of a body, known as the capacitor, to store electrical charge. The SI unit for capacitance is Farad (F) but usually it will be expressed in smaller subunits such as pF. For a parallel plate capacitor as shown in Figure 2.4 above, firstly alternating current is allowed to flow through the two electrodes. Then the

accumulation of positive and negative charges (q) and potential difference (V) will result in capacitance as shown in Eq. (2.3) below [21].

$$C = \frac{q}{V} \tag{2.3}$$

Based on the concept of electrostatic analysis, capacitance, C can be calculated using

$$C = \frac{\varepsilon * \varepsilon_a * A}{d} \tag{2.4}$$

where ε is the electric constant (8.854×10^{-12} F.m^{-1}), ε_a is the dielectric constant or permittivity of the dielectric material, A is the area of the plates and d is the separation distance between the two plates.

The difference in permittivity of fluids in two-phase flow like oil and water allows capacitance method to be applied easily in phase volume fraction measurement on oil pipelines. With constant pipe thickness, A and d of capacitors, the focus of this project is on the effect of dielectric constant on capacitance. Table 2.2 below summarizes the general electrical properties of oil and water where the large contrast in dielectric constant is a great advantage in this method.

Table 2.2: Comparison on electrical properties of fluids [20]

Properties	**Oil**	**Tap water [17]**	**Distilled water [17]**
Permittivity, ε_a	2 - 3	78.5	81
Conductivity	None	High	Low

The result of capacitance method depends on conductivity of fluids [20]. Generally, oil is non-conductive while water is conductive. Non-conductive fluid is preferable as there will not be electrical losses during the measurement of water content that will affect the capacitance value measured. Thus, distilled water with lower conductivity will be selected instead of tap water due to its lower conductivity. In terms of permittivity, with the large difference of permittivity of about $\Delta\varepsilon_a$ = 81 – 2 = 79, slight variation in water in oil-water mixture is expected to result in change in effective permittivity and thus capacitance which is large enough to be detected by the electrodes [20].

2.2 Oil-water flow and water content measurement

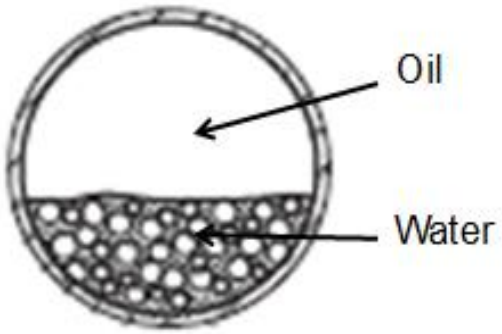

Figure 2.5: Oil-water mixture in a pipe [22]

According to Ahmad et al, two-phase flow is defined as the simultaneous flow of two immiscible liquids in pipes [23]. This flow exists in natural phenomena such as bubbles, rain, sea waves and fountain. A good example of liquid-liquid flow is the mixture of two different fluids, i.e. oil and water in a pipe as illustrated in Figure 2.5 above. [24].

Table 2.3: Physical properties of water and oil [25]

Properties	Water	Oil (SAE 40)
Density (kg/m³)	1000	890
Viscosity (Pa·s)	0.001	0.107
Surface tension (N/m)	0.072	0.032
Interfacial tension (oil-water) (N/m)	0.024	-

Among all physical properties of oil and water as listed down in Table 2.3 above, it should be noted that water (1000 kg/m³) has higher density than oil (about 800 kg/m³) and thus it will always form the lower layer below oil in stratified flow [25]. The differences in other physical properties will not have significant impact on the two-phase flow of oil and water. This flow can be categorized into dynamic flow or static flow. The former refers to the fluids which are moving at certain velocities while the latter refers to the fluids which are stationary or with zero velocity.

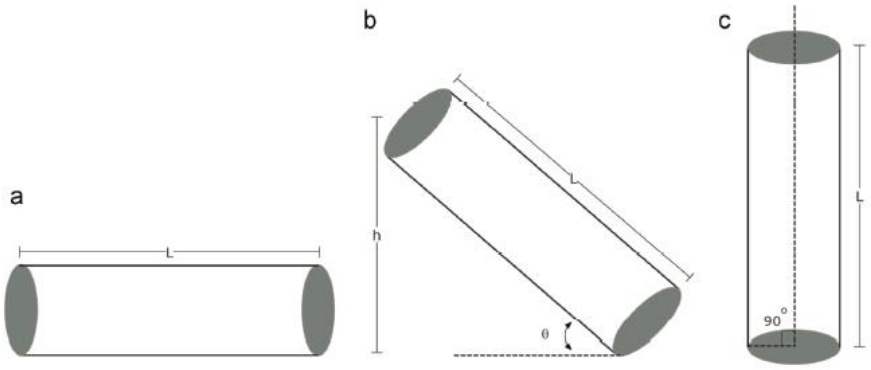

Figure 2.6: Typical positions of pipeline [23]

To allow the flow of two-phase fluids from one end to another, the pipe can be placed in three different positions as illustrated in Figure 2.6 above where each of them will result in different flow patterns [23]. In most of the cases, horizontal two-phase flow is applied.

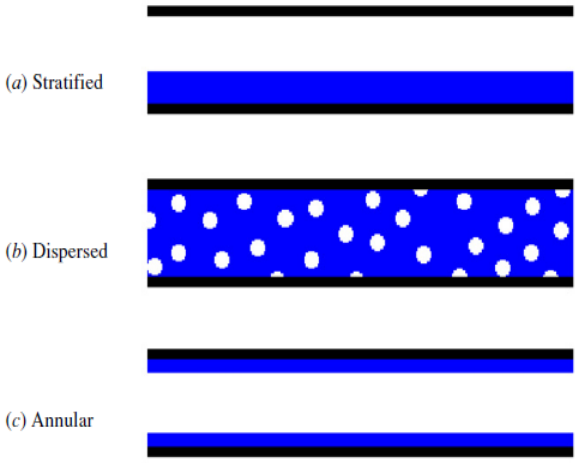

Figure 2.7: Typical types of two-phase flow [9]

The types of flow in two-phase mixture include stratified flow, plug flow, slug flow, dispersed flow (either oil in water or water in oil) and annular flow with some of them illustrated in Figure 2.7 above [9]. For the case of zero-velocity static flow, stratified flow is found out to be the most typical flow in the pipe.

For the experiment regarding two phase flow of moving fluids, the setup consists of 3 main parts namely oil section, water section and test section as illustrated in Figure 2.8 below. Among the apparatus and devices involved are oil tank, water tank, rheometer,

rotameter, pipe, separation vessel and coaleser [23]. Meanwhile for the experiment of static two phase flow, the setup is rather simpler with manual insertion of fluids into the pipe using only syringe and beaker for volume measurement. For better accuracy of measurement, the surrounding temperature should be kept constant to avoid any influence on physical properties of fluids during the experiment.

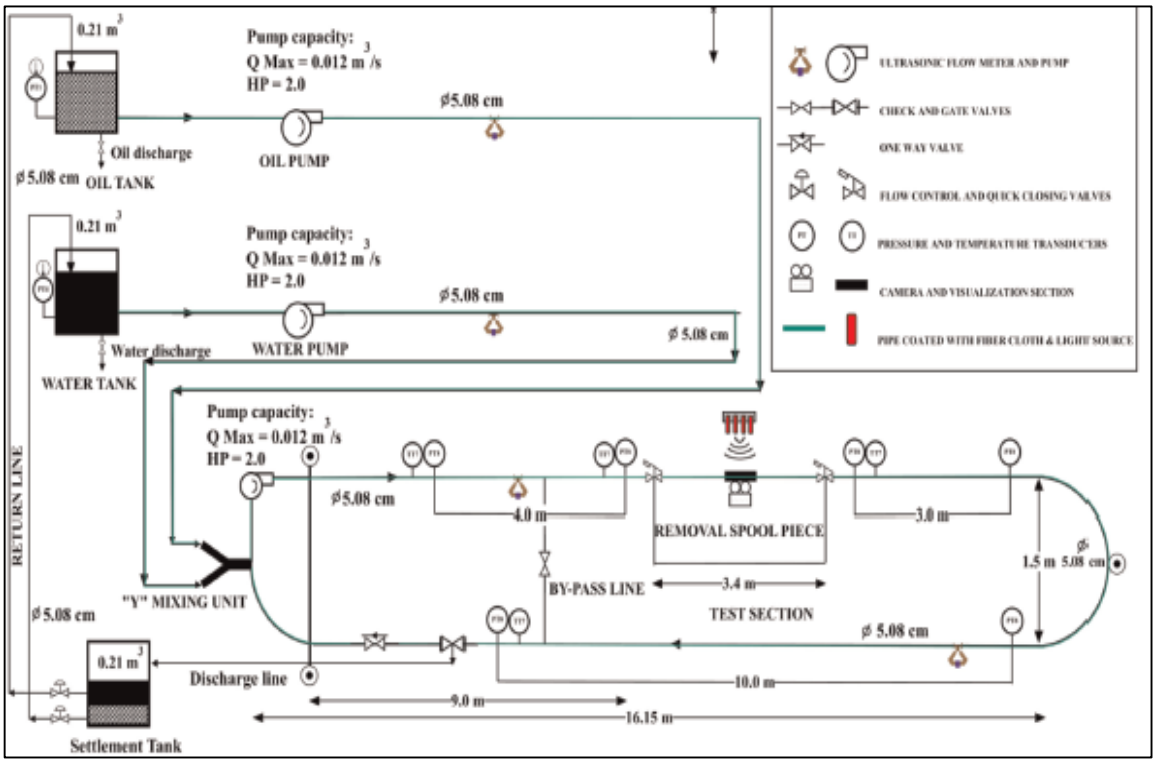

Figure 2.8: Typical experimental setup for oil-water flow [22]

Capacitance method is widely used in industry for applications like position sensing, liquid level sensing and pressure sensing [6]. For those cases, the capacitance changes are significant enough to be measured by the electrodes. However, for the detection of water content in oil-water mixture, it might involve only minor changes in water concentration which is not enough to be detected by the electrodes [26]. Hence, a simple capacitance interface circuit as shown in Figure 2.9 below will be applied to amplify the capacitance. As a result of amplification, the capacitance will be automatically converted into voltage as the output. This circuit is immune from stray capacitance besides having high sensitivity and accuracy as proven by Maher [26] and Preethichandra [6].

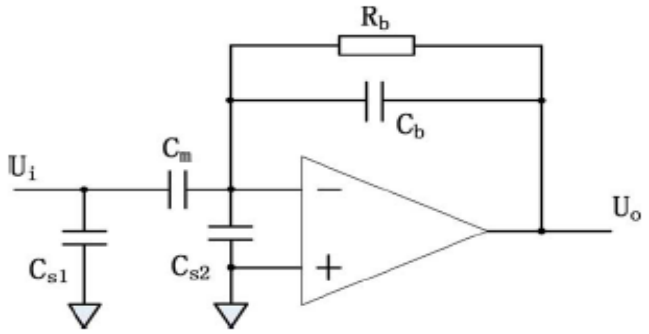

Figure 2.9: Simplified capacitance interface circuit [27]

As mentioned by Ye et al. [27], the conversion from capacitance to voltage is based on charge transfer principle where the output voltage, U_o can be calculated using

$$U_o = \frac{j\,\omega\,C_m R_b}{1+ j\,\omega\,C_b R_b}\,U_i \tag{2.5}$$

where U_i is the input voltage, ω is the angular frequency of the input voltage, C_m is the unknown capacitance to be determined. From Eq. (2.5) above, the output voltage is directly proportional to the capacitance of oil-water mixture. This finding is important in analysis of result due to the fact that for any increment in water content in oil-water mixture, it is expected to have is an increase in the voltage measured or the capacitance.

In the research carried by A.Maher and Z.A.Muhammad to design the interface circuit for accurate measurement of water content in crude oil [19], the linear relationship between output voltage obtained and capacitance had been proven via the outcomes of two graphs as illustrated in Figure 2.10 and Figure 2.11 below, respectively.

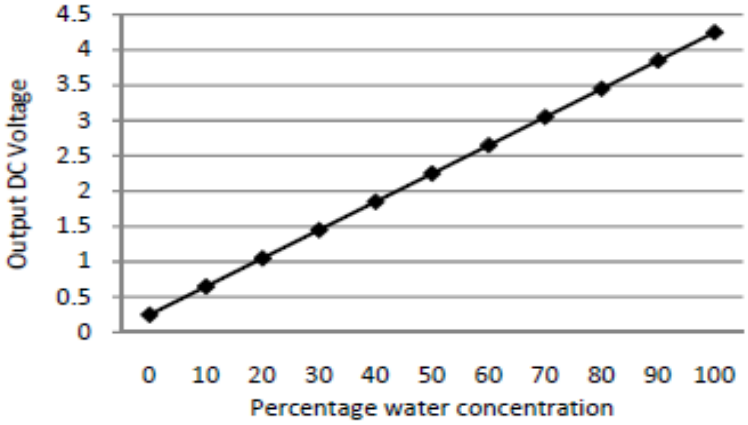

Figure 2.10: Graph of voltage vs. percentage water concentration [26]

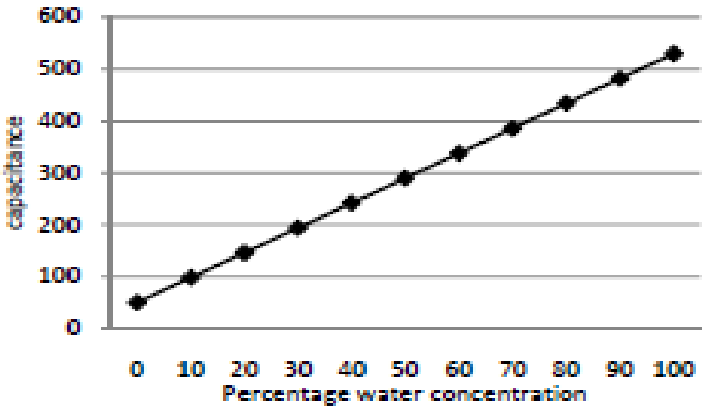

Figure 2.11: Graph of capacitance vs. percentage water concentration [26]

During the water volume fraction measurement experiment, as proposed by Domenico [18], an insulator pipe made up of materials such as Plexiglass should be used to prevent or minimize the electrical loss due to conductivity effect during the implementation of capacitance method. Another typical material is known as Polyvinyl chloride (PVC) which is commonly adopted by most of the previous researchers.

2.3 Configurations of electrodes

In capacitance method used for pipeline inspection, electrodes, also known as capacitive sensors, are normally mounted around the pipe test section. Typically, two electrodes will be used simultaneously together with guards and shielding connected to a capacitance interface circuit [8]. Some of the common configurations are double rings electrodes, concave electrodes, and helical electrodes as illustrated in Figure 2.12, Figure 2.13 and Figure 2.14 respectively below [5].

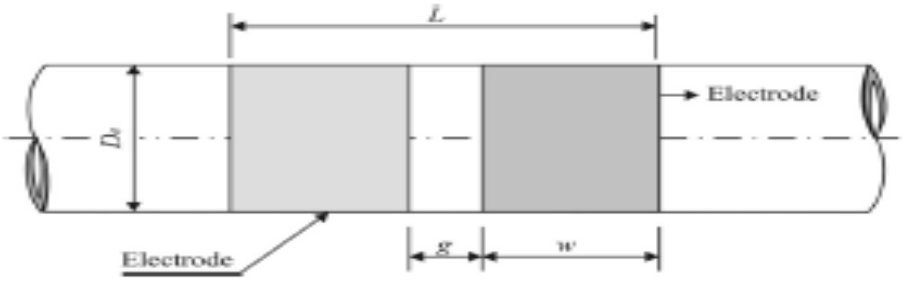

Figure 2.12: Double rings electrodes' sensor [5]

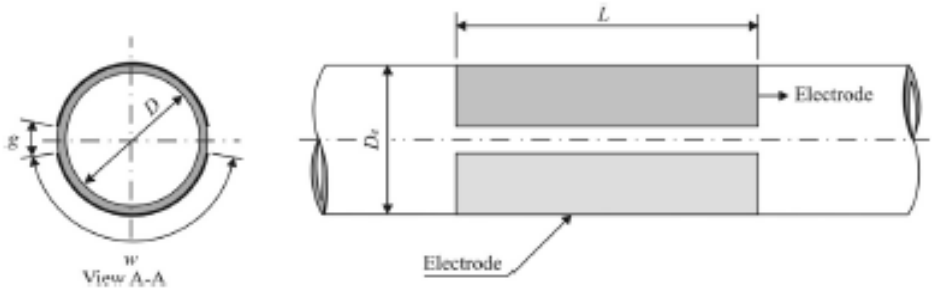

Figure 2.13: Concave electrodes' sensor [5]

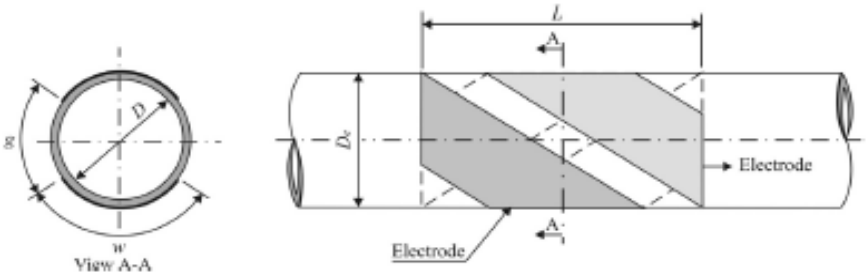

Figure 2.14: 180˚ helical electrodes' sensor [5]

Also, as one of the parameters in determination of capacitance as shown in Eq. (2.4), the area of electrodes in contact with the pipe wall should be made constant during the comparison of performance for different electrodes configurations. This is to make sure that the capability of sensing the change in capacitance is equal for all configurations. During the experiment done by Emerson and Diego [5] to measure the volumetric concentration in two-phase flows, the dimensions of all configurations had been designed as shown in Table 2.4 below. It should be noted that separate experiments on those configurations were carried out on the similar pipe.

Table 2.4: Dimensions of capacitive sensors [5]

Sensor	*L* [mm]	*w* [mm] (°)	*g* [mm] (°)
Helical	105.2	60.1 (171.4)	16.3 (23.2)
Concave	98.0	55.0 (156.8)	4.29 (6.1)
Double ring	105.0	47.0	11.0

Meanwhile, for electrodes with helical configuration, it has been shown that the measurement error due to the effect of flow regime and dependency on angle of orientation can be minimized by helical electrodes with 180˚ or 360˚ angle of twisting [19]. This phenomenon was proven by Jarle and Erling in their experiment.

Different configurations of electrodes will produce different results as water content increases in oil-water mixture. This is due to different positions of wrapping of electrodes around the pipes relative to the oil-water mixture that affect the detection ability of capacitor sensors. The trend of previous studies is found to be as follow:

i. Focusing on the comparison of performance for different combination of fluids inside the pipe, e.g. gas-water and gas-oil. [19]
ii. Focusing on analysis on the performance of a single configuration of electrodes.

For example, the performance of helical (double helix) capacitance sensors had been investigated by Zhai et al. in their experiment of liquid holdup measurement in horizontal oil-water two-phase flow pipes [28]. The response of sensors in terms of normalised voltages, V_N towards the volume ratio of oil or oil holdup for different types of flows with constant superficial velocities had been recorded.

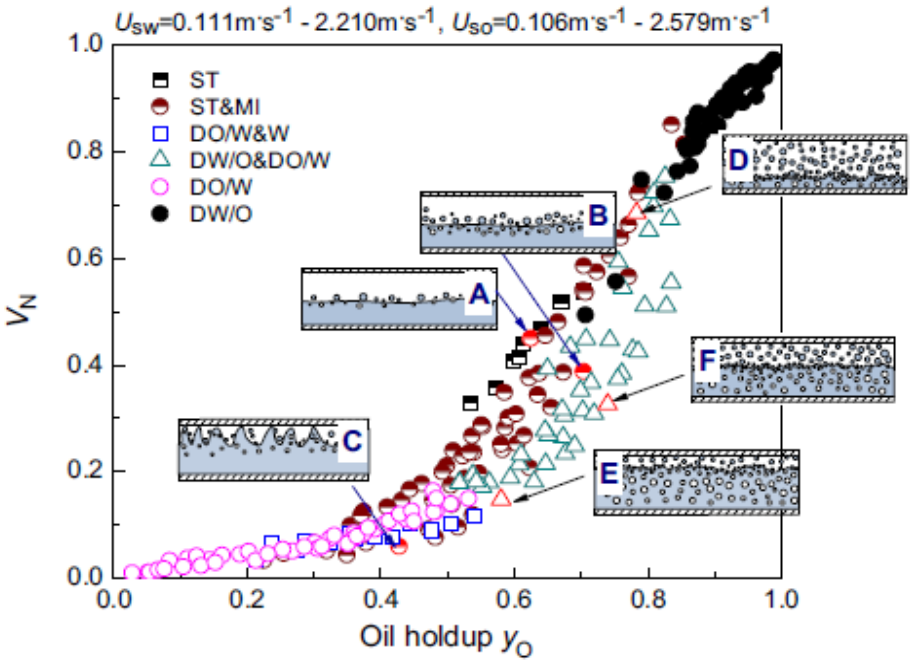

Figure 2.15: Characteristics of double helix sensor in oil holdup measurement [28]

Assessment on the performance each configuration can be carried out in terms of linearity of response which is measurable and comparable [5]. Ideally, a good configuration is expected to produce the capacitance result with high linearity of response, i.e. directly proportional relationship between capacitance and volume ratio of water in oil-water mixture as illustrated in Figure 2.16 below.

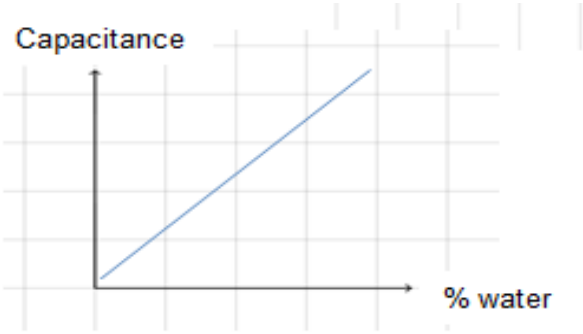

Figure 2.16: Ideal result for capacitance method [26]

2.4 Sensitivity of electrodes

Besides linearity of response, configurations of electrodes can also be accessed in terms of sensitivity of electrodes or capacitance sensors. Many previous studies have been carried out where concave capacitance sensor was found to have the higher sensitivity compared to double rings and helical electrodes [29-31]. Also, the sensitivity distribution of concave capacitance sensor had been heavily studied by Xie et al. [32] who proposed the huge influence of pipe wall thickness on the sensitivity result.

In a research done by Caniere et al. [20, 33], different flow patterns had been identified by using a concave capacitance sensor. Meanwhile, a calibration method for concave capacitance sensor has been suggested by Kerpel et al. [34] in measuring the phase volume fraction in two-phase flow. The distribution of element sensitivity field forms a sensitivity field for the whole measurement region. The measurement field of the sensor is meshed into several small elements by using the finite element method (FEM), in which the sensitivity of element i can be expressed as

$$S(i) = \frac{C(i)-C(\varepsilon_l)}{C(\varepsilon_h)-C(\varepsilon_l)} \; x \; \frac{V}{V_i} \qquad (2.6)$$

where $S(i)$ is the sensitivity of the ith element, $C(\varepsilon_l)$ is the capacitance between exciting and measurement electrode while the permittivity or dielectric constant of all the elements in measurement region is ε_l. $C(\varepsilon_h)$ is the capacitance between the two electrodes while the permittivity of all the elements in the measurement region is ε_h. $C(i)$ is the capacitance between the two electrodes while the permittivity of the ith element is ε_h and the dielectric constant of other elements is ε_l. Also, V represents the total volume of detection region while V_i represents the volume of the ith element.

In order to describe the sensitivity field homogeneity and obtain the capacitance variation with respect to the change of permittivity distribution, the sensitivity variation parameter based on the element sensitivity is defined as

$$SVP = \frac{S_{dev}}{S_{avg}}\ x\ 100\% \tag{2.7}$$

where S_{avg} is the average value of all the element sensitivities which is expressed as

$$S_{avg} = \frac{1}{M}\sum_{i=1}^{M} S(i) \tag{2.8}$$

and S_{dev} is the standard deviation of element sensitivities in the measurement region which can be expressed as:

$$S_{dev} = \left[\frac{1}{M}\sum_{i=1}^{M}\left(S(i) - S_{avg}\right)^2\right]^{1/2} \tag{2.9}$$

where M represents the total number of elements in the measurement region.

The ideal case in sensitivity analysis is always to achieve maximum S_{avg} that represents the detection ability for a certain amount of change in capacitance. At the same time, the SVP values should be minimised so that the measurement results are less affected by the flow pattern, i.e. higher homogeneity or linearity of results. In other words, the results will be more independent of the location of the equal-volume element i throughout the measurement region of the two-phase fluid.

In the approach done by Zhao et al. to carry out liquid holdup measurement in horizontal oil–water two-phase flow, the performance of concave capacitance sensor had been evaluated in terms of sensitivity [35]. The 2D sensitivity distribution of the electrodes

was performed by dividing the radial section of the pipe into 128 elements as illustrated in Figure 2.17 below.

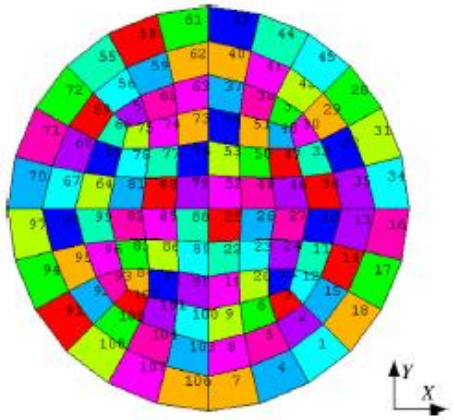

Figure 2.17: The 2D mapping grid structure of fluid [35]

In this experiment, oil-water flow was analysed with the permittivity of water, $\mathcal{E}$ = 80 and the permittivity of oil $\mathcal{E}_o$ = 2.5. With that, the sensitivity of each element can be calculated as well as the sensitivity distribution of the capacitance sensors. In order to ensure the accuracy of the finite element calculation, the electrode edge region is meshed in refined grids. As the results, the change in S_{avg} and SVP for different angles of electrodes had been recorded as shown in Figure 2.18 below.

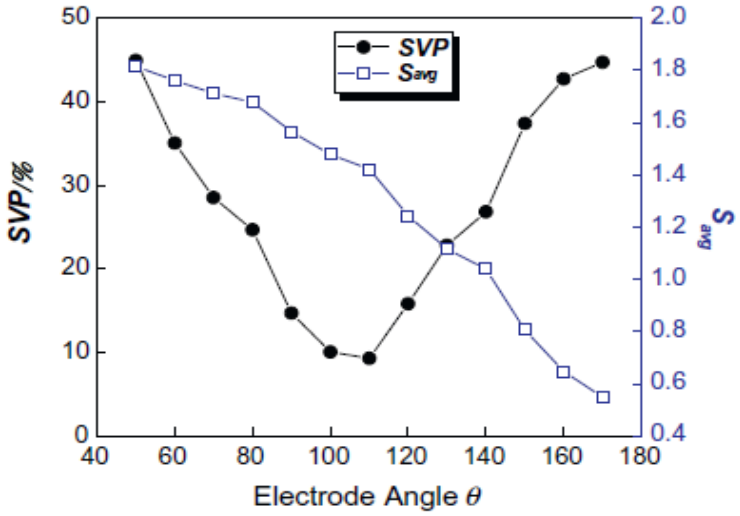

Figure 2.18: The effect of electrode angle on sensor sensitivity distribution [35]

CHAPTER 3
METHODOLOGY

3.1 Methodology flow chart

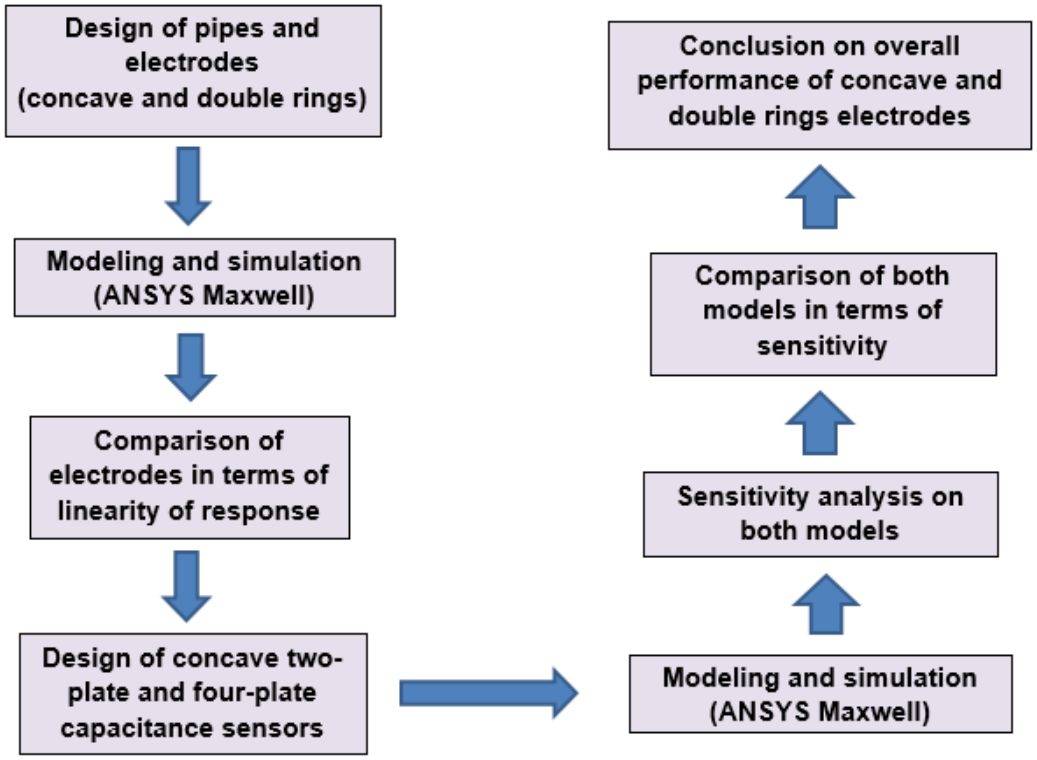

Figure 3.1: General flow chart of the project

This project will be started up with the design of pipes and electrodes. Similar pipes will be designed to be complemented with different configurations of electrodes. After the identification of design parameters, the pipes and electrodes namely concave electrodes and double rings electrodes will be modeled using ANSYS Maxwell software with several boundary conditions taken into consideration. From the analysis on the simulation results, the better configuration of electrode will then be identified based on the linearity of response towards different oil-water content.

Next, sensitivity analysis will be performed on the concave electrodes to compare the conventional two-plate model and the proposed four-plate model. During the sensitivity analysis, two parameters i.e. sensor relative sensitivity and sensitivity variation parameter will be used to identify the design parameters that produce the best result Based on the capacitance measurement results with respect to linearity of response and sensitivity of electrodes, the overall performance of concave electrodes and double rings electrodes can then be evaluated separately to come up with an appropriate conclusion.

3.2 Gantt chart

The steps involved have been listed down in a Gantt chart with key milestones included.

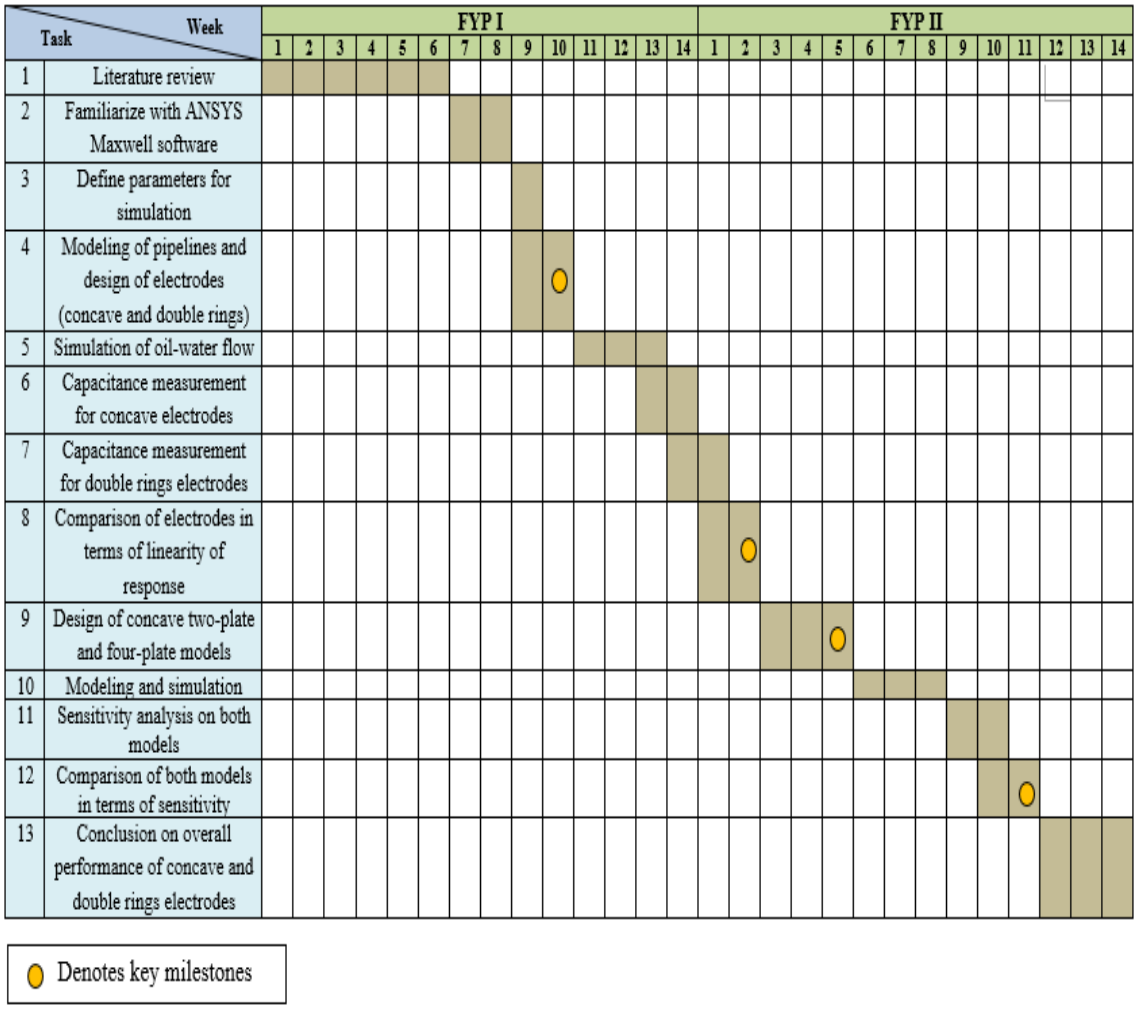

Figure 3.2: Gantt chart of the project with milestones

3.3 Project Methodology

In this project, simulation will be carried out using ANSYS Maxwell where it is categorized into two main sections, i.e. analysis on the linearity of response of concave and double rings electrodes followed by sensitivity analysis on concave electrodes.

3.3.1 Design of pipes and electrodes

The design of pipes and electrodes involve several important parameters that need to be taken into consideration. By referring to the different views of the pipe-electrode configuration as shown in Figure 3.3 below, the parameters are generally as follow:

i. Length of pipe (L_p)
ii. Internal diameter of pipe (D) and internal radius of pipe (r)
iii. External diameter of pipe (D_e) and external radius of pipe (r_e)
iv. Axial length of electrodes (L)
v. Width /angle of width of electrodes (w)
vi. Separation distance/angle between electrodes (g)

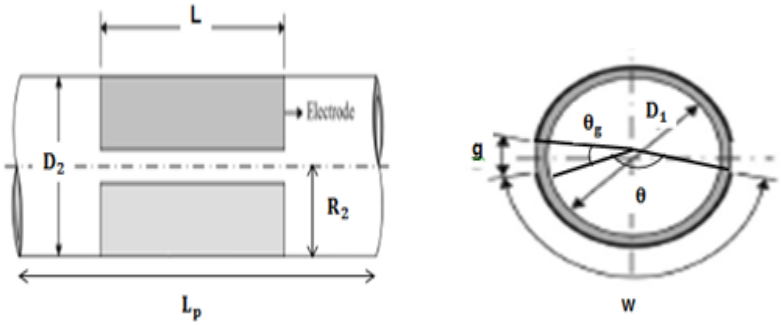

Figure 3.3: Illustration of design parameters [5]

3.3.2 Linearity of response

To compare the performance of different configurations of electrodes, the pipes used in the simulation have to be similar in dimensions. Their design parameters are shown in Table 3.1 below. Meanwhile, the area of electrodes in contact with pipe wall should be

constant as it is the region responsible for detection of capacitance changes in oil-water mixture. In this project, all the electrodes are made of copper and having the similar thickness of 0.5 mm with all resulting in almost similar frontal area of about 0.006 m².

Table 3.1: Design parameters of pipes

Parameters	Remarks
Material of pipe	PVC plastic
Length of pipe, L_p	150 mm
Internal diameter of pipe, D_1	33.85 mm
Internal radius of pipe, R_1	16.925 mm
External diameter of pipe, D_2	40.2 mm
External radius of pipe, R_2	20.1 mm

3.3.2.1 Concave electrodes

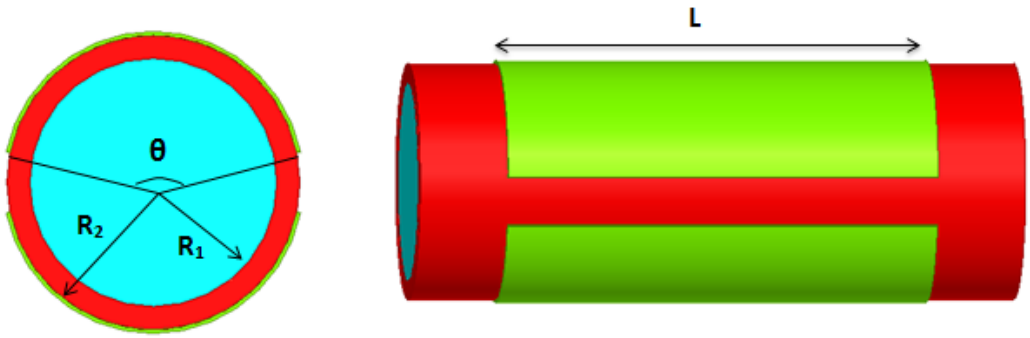

Figure 3.4: Design of concave electrodes

Table 3.2: Design parameters of concave electrodes

Parameters	Remarks
Material of electrodes	Copper
Thickness of electrodes	0.5 mm
Axial length of electrodes, L	98 mm
Angle of electrodes, θ	156.8˚ or 2.737 rad

3.3.2.2 Double rings electrodes

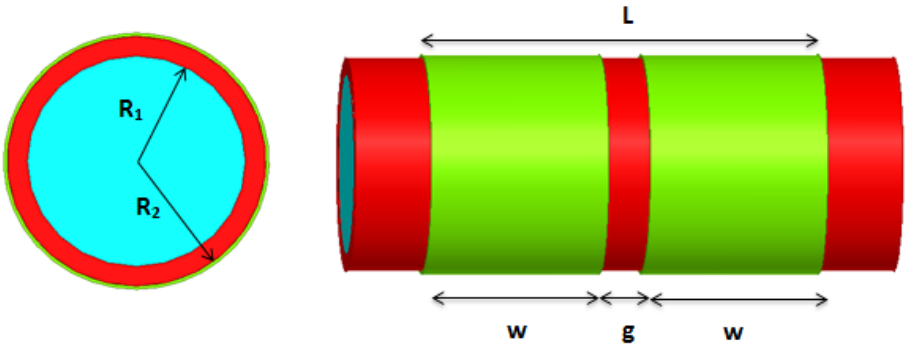

Figure 3.5: Design of double rings electrodes

Table 3.3: Design parameters of double rings electrodes

Parameters	Remarks
Material of electrodes	Copper
Thickness of electrodes	0.5 mm
Axial length of electrodes, L	105 mm
Width of electrodes, w	47 mm
Separation distance, g	11 mm

3.3.2.3 Modeling and simulation

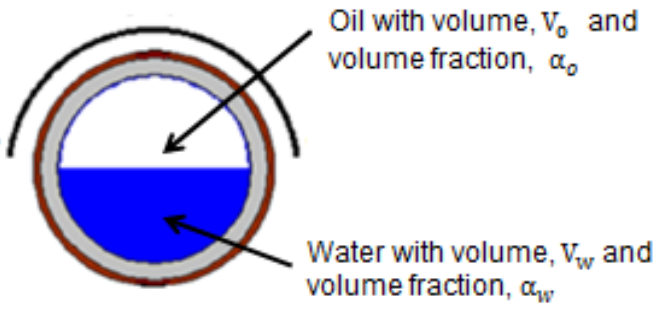

Figure 3.6: Stratified oil-water mixture [5]

Based on the designs finalised, ANSYS Maxwell will be used to generate the three-dimensional (3D) models of the pipes and electrodes. Before performing the modeling, it should be noted that the length of the pipes L_p is designed to be equal to the axial length

of electrodes, L. Also, the basic information on the models and the electrical properties of materials have been listed down in Table 3.4 and Table 3.5 respectively below.

Table 3.4: Basic information on ANSYS modeling

Parameters	Remarks
Type of fluids	Oil and distilled water
Type of mixture	Stratified
Type of flow	Static (Horizontal pipe)
Velocity of fluids	0 m/s

Table 3.5: Electrical properties of all components

Components	Materials	Relative permittivity	Bulk conductivity (siemens/m)
Fluid 1	Oil	3	0
Fluid 2	Distilled water	81	0.0002
Pipes	PVC plastic	2.7	0
Electrodes	Copper	1	58000000

In ANSYS modeling, the manipulating variable is the water content or specifically, the volume ratio of water in the pipe. For increasing volume ratio of water, the cross-sectional area of volume occupied by water as well as the height of the area, as illustrated in side-viewed Figure 3.7 below, increases. It should be noted that in this project, the height of water, h is an important parameter for the modeling of water.

A methodology has been formulated to calculate h for varying volume ratio of water in the pipe as shown in Table 3.6 below. Also, for step number 4, the central angle of water, θ can be solved using Microsoft Excel through iteration method. Since all electrodes configurations have constant internal radius of pipes, the height of water, h for volume ratio of water in all cases will remain constant. The values of h for each volume ratio can be determined and are tabulated in Table 3.7 below.

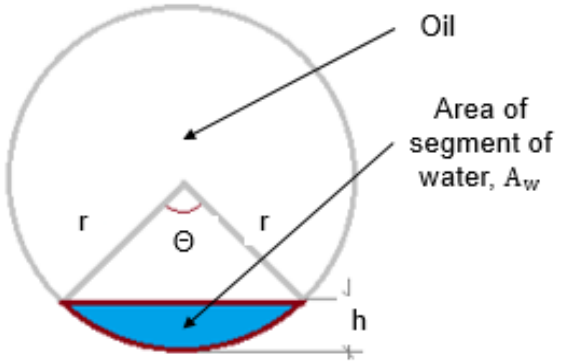

Figure 3.7: Illustration on height of water, h

Table 3.6: Methodology to calculate the height of water, h

Step	Parameters	Formulae
1	Total volume of fluid	$V_T = \pi r^2 x L$
2	Volume of water	$V_w = \alpha_w x V_T$
3	Cross-sectional area of water	$A_w = \frac{V_w}{L}$
4	Central angle	$\theta - sin\ \theta = \frac{2A_w}{r^2}$ $\theta\ (rad) = ?$
5	Height of water	$h = r\ (1 - cos\ \frac{\theta}{2})$

Table 3.7: Calculated h values for all volume ratios of water

Volume ratio of water, α_w	Height of water, h (mm)
0.00	0.000
0.10	5.297
0.20	8.600
0.30	11.519
0.40	14.750
0.50	16.925
0.60	19.100
0.70	22.331
0.80	25.250

0.90	28.553
1.00	33.850

After the modeling of electrodes, it will be the stage of simulation on the models with varying water content. The common input variables for the simulation in ANSYS Maxwell are identified and listed down in Table 3.8 below.

Table 3.8: Input variables for simulation

Input	**Remarks**
Solution type	Electrostatic
Boundaries	None
Excitations	i. 1 V for electrode 1 (voltage 1) ii. 0 V for electrode 2 (voltage 2)
Parameters	Matrix for voltage 1 and voltage 2

At this stage, the simulation can be performed with procedures as follow:

1. The pipe with concave electrodes is fully filled with oil and the capacitance value for $\alpha_w = 0$, C_1 is recorded.
2. The same pipe is then fully filled with distilled water and the capacitance value for $\alpha_w = 1$, C_2 is recorded.
3. Distilled water is added into the oil with increasing volume ratio of water, i.e. α_w = 0.1, 0.2, 0.3, 0.4, 0.5, 0.6, 0.7, 0.8 and 0.9.
4. The capacitance values for all volume fractions of water are recorded
5. All the capacitance values obtained are converted into normalised capacitance, C_N which is between 0 and 1, having the same range as α_w.
6. The results obtained are plotted in a graph of C_N vs. α_w and are compared to the ideal linear graph constructed from the values of C_1 and C_2.
7. The absolute errors for all α_w and the mean absolute error are computed.
8. Steps 1–7 are repeated for pipes with double rings electrodes.
9. The mean absolute errors for both configurations of electrodes will be compared.

3.3.3 Sensitivity analysis on concave electrodes

The design parameters for concave electrodes and pipes are shown in Table 3.9 below. It should be noted that in this case, the dimension of pipes used is different from that for analysis on linearity of response in previous section. Also, the electrical properties of materials have been listed down in Table 3.10 below.

Table 3.9: Design parameters of concave electrodes

Parameters	**Remarks**
Number of electrode plates	2 or 4
Material of electrodes	Copper
Thickness of electrodes	0.5 mm
Length of electrode, L	3 mm
Material of pipe	Plexiglass
Internal diameter of pipe, D_1	16.02 mm
Internal radius of pipe, R_1	8.01 mm
External diameter of pipe, D_2	20 mm
External radius of pipe, R_2	10 mm

Table 3.10: Electrical properties of all components

Components	**Materials**	**Relative permittivity**	**Bulk conductivity (siemens/m)**
Fluid 1	Oil	2	0
Fluid 2	Distilled water	81	0.0002
Pipe	Plexiglass	3.4	0
Electrodes	Copper	1	58000000

Besides the conventional way of designing the concave electrodes in two-plate configuration, the electrodes can be divided into several other numbers of plates as well. In this section, the two-plate and four-plate capacitive sensors will be investigated and compared in terms of the average sensitivity and sensitivity variation parameters.

The design configuration of two-plate and four-plate capacitance sensor has been illustrated in Figure 3.8 and Figure 3.9, respectively. As shown in Figure 3.8, the conventional concave capacitance sensor consists of only two plates, namely measuring electrode and exciting electrode. Meanwhile, Figure 3.9 shows the four-plate concave capacitance sensor which consists of two measuring electrodes and two exciting electrodes. It should be noted that the concave plates are always placed alternately with measuring and exciting electrodes. The electric field is formed between exciting and measuring electrode where an AC voltage is applied. Typically, 0V is applied on measuring electrode while 1V is applied on exciting electrode.

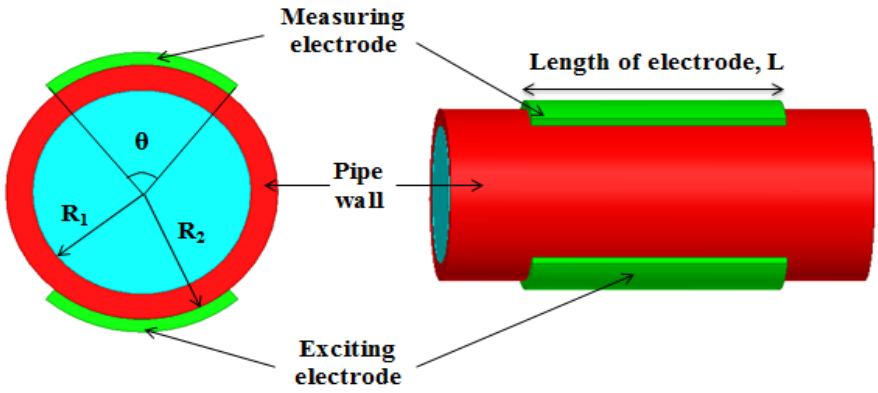

Figure 3.8: Design of two-plate concave electrodes

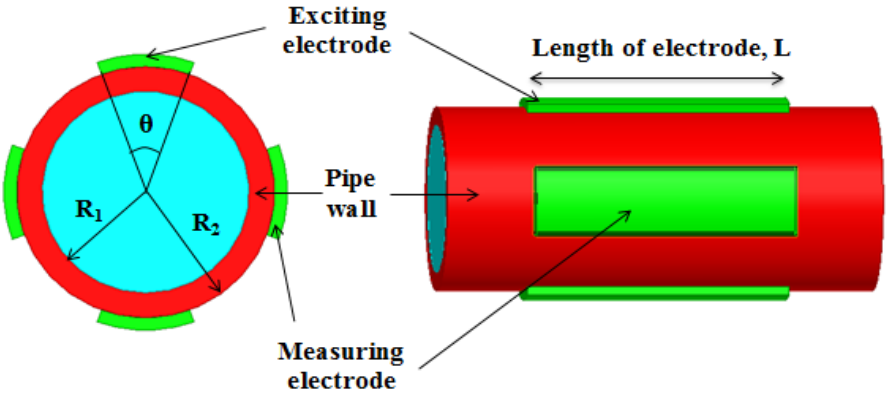

Figure 3.9: Design of four-plate concave electrodes

The calculation methodology of the sensitivity analysis on both two-plate and four-plate models will be summarized as shown in Table 3.11 below.

Table 3.11: Calculation steps for sensitivity analysis

Step	Parameter	Formulae
1	Sensitivity of elements	$S(i) = \frac{C(i) - C(\varepsilon_l)}{C(\varepsilon_h) - C(\varepsilon_l)} \; x \; \frac{V}{V_i}$
2	Sensor relative sensitivity	$S_{avg} = \frac{1}{M} \sum_{i=1}^{M} S(i)$
3	Standard deviation of sensitivity	$S_{dev} = [\, \frac{1}{M} \sum_{i=1}^{M} (S(i) - S_{avg})^2 \,]^{1/2}$
4	Sensitivity variation parameter	$SVP = \frac{S_{dev}}{S_{avg}} \; x \; 100\%$

In this case, the two-phase flow is set to be oil-water flow. Also, the measurement region of the fluid is divided into a total of 246 elements. The parameters of sensitivity analysis had been identified and listed down in Table 3.12 below.

Table 3.12: Parameters of sensitivity analysis

Parameters	Remarks
Permittivity, ε_l	2 (oil)
Permittivity, ε_h	81 (distilled water)
Number of elements, M	246
Shape of elements	Cylinder
Volume of each element, V_i	2.3562 mm³
Total volume of fluid, V	604.6947 mm³

The division of the fluid into small water elements can be illustrated as shown in Figure 3.10 below while the location of all elements is indicated in Table 3.13 below. For all 21

starting positions, the elements will be positioned downwards along the y-axis to form a total of 246 water elements in the oil.

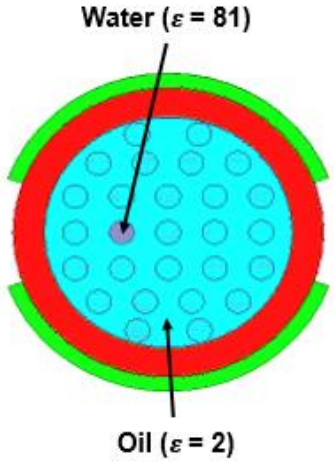

Figure 3.10: Distribution of elements in the pipe

Table 3.13: Location of all elements in the pipe

Point	Coordinate (x , y)	Elements
1	(0 , 7.5)	1 - 16
2	(0.8, 7.3)	17 - 32
3	(1.6 , 7.1)	33 - 48
4	(2.4 , 6.9)	49 - 63
5	(3.2 , 6.7)	64 - 78
6	(4.0 , 6.3)	79 - 92
7	(4.8 , 5.6)	93 - 105
8	(5.6 , 4.9)	106 - 116
9	(6.4 , 3.8)	117 - 125
10	(7.2 , 1.9)	126 - 130
11	(7.5 , 0)	131
12	(-0.8, 7.3)	132 - 147
13	(-1.6 , 7.1)	148 - 163
14	(-2.4 , 6.9)	164 - 178
15	(-3.2 , 6.7)	179 - 193
16	(-4.0 , 6.3)	194 - 207
17	(-4.8 , 5.6)	208 - 220
18	(-5.6 , 4.9)	221 - 231
19	(-6.4 , 3.8)	232 - 240
20	(-7.2 , 1.9)	241 - 245
21	(-7.5 , 0)	246

By manipulating the θ, the surface area of two-plate sensor and four-phase sensor can be made equivalent easily for comparison purpose in this paper. The opening angle for four-plate sensor is always half of that of equal-area two-plate sensor. ANSYS Maxwell software is utilised for simulation of the two-phase flow in order to obtain the capacitance values for all locations of element in the measurement region.

With that, based on the formulas stated in Table 3.11, for two-plate concave capacitance sensors, both S_{avg} and SVP values are calculated for different angles of electrodes ranging from θ = 60˚ to θ = 160˚ with an incremental of 10˚ each time. Similarly, for four-plate concave capacitance sensors, S_{avg} and SVP values are calculated for different angles of electrodes ranging from θ = 30˚ to θ = 80˚ with an incremental of 5˚ each time. The summary of the equivalent angles of electrodes adopted for simulation of both models is shown in Table 3.14 below.

Table 3.14: Summary of equivalent angles of electrodes for simulation

Angles for two-plate model, θ	**Angles for four-plate model, θ**
60˚	30˚
70˚	35˚
80˚	40˚
90˚	45˚
100˚	50˚
110˚	55˚
120˚	60˚
130˚	65˚
140˚	70˚
150˚	75˚
160˚	80˚

CHAPTER 4
RESULTS AND DISCUSSION

4.1 Linearity of response

The linearity of response of concave electrodes and double rings electrodes will be evaluated separately before their results are put into comparison.

4.1.1 Concave electrodes

The initial capacitance values for concave model with fully filled oil and fully filled distilled water are shown in Table 4.1 below. Also, the normalised capacitance values, C_N from $\alpha_w = 0.1$ up to $\alpha_w = 0.9$ are obtained and listed down in Table 4.2 below.

Table 4.1: Initial capacitance values for concave electrodes

Symbol	Volume ratio of water, α_w	Capacitance, C (pF)
C_1	0.00	4.7858
C_2	1.00	17.002

Table 4.2: Simulation results for concave electrodes

Volume ratio of water, α_w	Capacitance, C (pF)	Normalised capacitance, C_N	Absolute error, E
0.10	4.9947	0.02	0.08
0.20	5.2420	0.04	0.16
0.30	5.6474	0.07	0.23
0.40	6.4757	0.14	0.26
0.50	7.3946	0.21	0.29

0.60	8.6808	0.32	0.28
0.70	11.0900	0.52	0.18
0.80	13.0620	0.68	0.12
0.90	14.9490	0.83	0.07

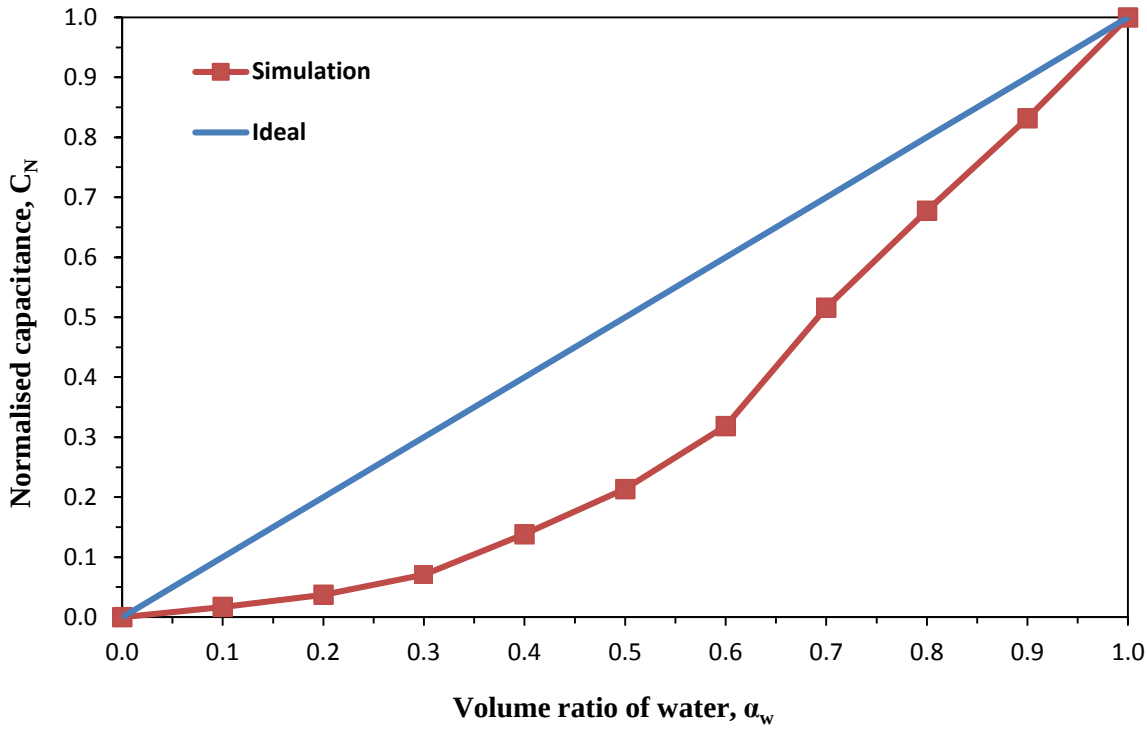

Figure 4.1: Graph of C_N vs. α_w for concave electrodes

The graph of normalised capacitance, C_N vs. volume ratio of water, α_w is plotted and presented in Figure 4.1 above where the simulation results are compared to the ideal results for concave electrodes. The change in normalised capacitance with varying volume ratio of water is found to be deviating significantly from the ideal case. However, the general trend is there where C_N increases with α_w.

From Table 4.2, the absolute errors of C_N for every value of α_w have been calculated and the mean absolute error is computed to be E= 0.186 or 18.6%.

4.1.2 Double rings electrodes

The initial capacitance values for double rings model with fully filled oil and fully filled distilled water are shown in Table 4.3 below. Also, the normalised capacitance values, C_N from $\alpha_w = 0.1$ up to $\alpha_w = 0.9$ are obtained and listed down in Table 4.4 below.

Table 4.3: Initial capacitance values for double rings electrodes

Symbol	Volume ratio of water, α_w	Capacitance, C (pF)
C_1	0.00	1.5213
C_2	1.00	9.7337

Table 4.4: Simulation results for double rings electrodes

Volume ratio of water, α_w	Capacitance, C (pF)	Normalised capacitance, C_N	Absolute error, E
0.10	2.8717	0.16	0.06
0.20	3.8043	0.28	0.08
0.30	4.6124	0.38	0.08
0.40	5.4794	0.48	0.08
0.50	6.0360	0.55	0.05
0.60	6.6052	0.62	0.02
0.70	7.3900	0.71	0.01
0.80	8.0835	0.80	0.00
0.90	8.8386	0.89	0.01

The graph of normalised capacitance, C_N vs. volume ratio of water, α_w is plotted and presented in Figure 4.2 below where the simulation results are compared to the ideal results for double rings electrodes. The change in normalised capacitance with varying volume ratio of water is found to be deviating slightly from the ideal case. Also, similar to the results for concave electrodes, the general trend is there where the C_N is found to be increasing with α_w.

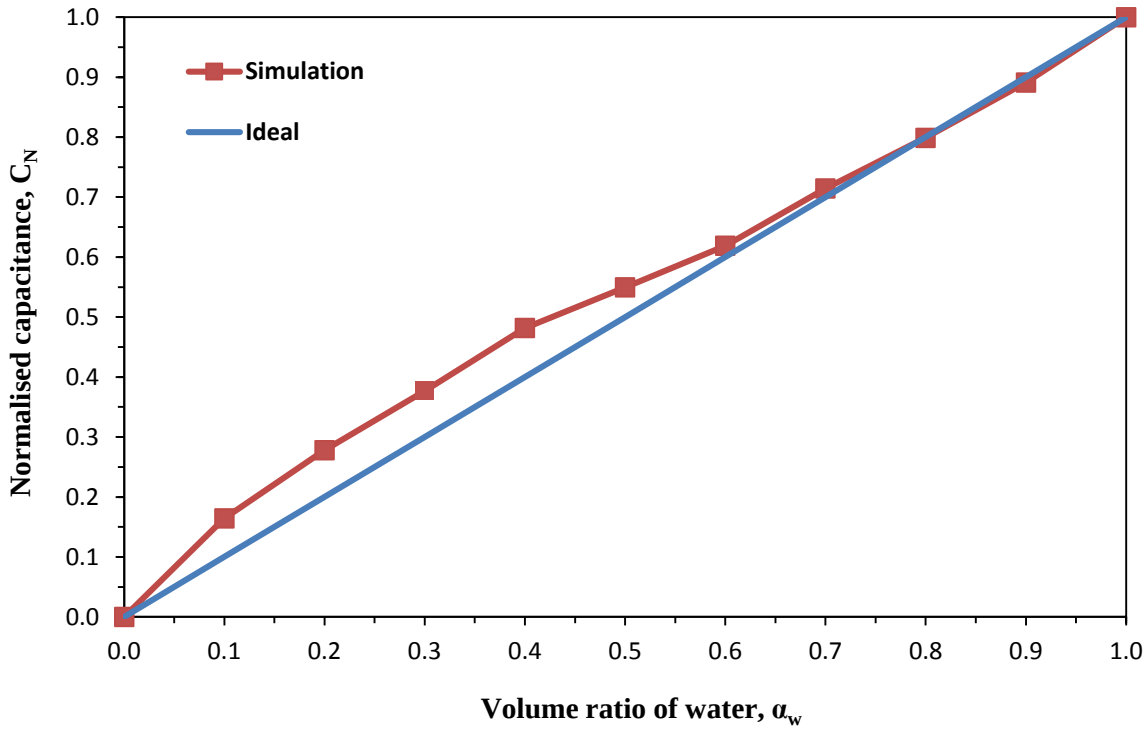

Figure 4.2: Graph of C_N vs. α_w for double rings electrodes

From Table 4.4, the absolute errors of C_N for every value of α_w have been calculated and the mean absolute error is computed to be E= 0.043 or 4.3%.

4.1.3 Comparison of performance

For every volume ratio of water, the normalized capacitance computed from concave electrodes and double rings electrodes have been listed down in Table 4.5 below.

Table 4.5: Comparison of results for concave and double rings electrodes

Volume ratio of water, α_w	**Normalized capacitance, C_N**	
	Concave electrodes	**Double rings electrodes**
0.10	0.02	0.16
0.20	0.04	0.28
0.30	0.07	0.38
0.40	0.14	0.48
0.50	0.21	0.55

0.60	0.32	0.62
0.70	0.52	0.71
0.80	0.68	0.80
0.90	0.83	0.89

From Table 4.5, it is obvious that for all volume ratio of water, the values of normalized capacitance for double rings electrodes are closer to the ideal values compared to that of concave electrodes. For better comparison, the graphs of C_N vs. α_w for both concave electrodes and double rings electrodes are illustrated in Figure 4.3 below.

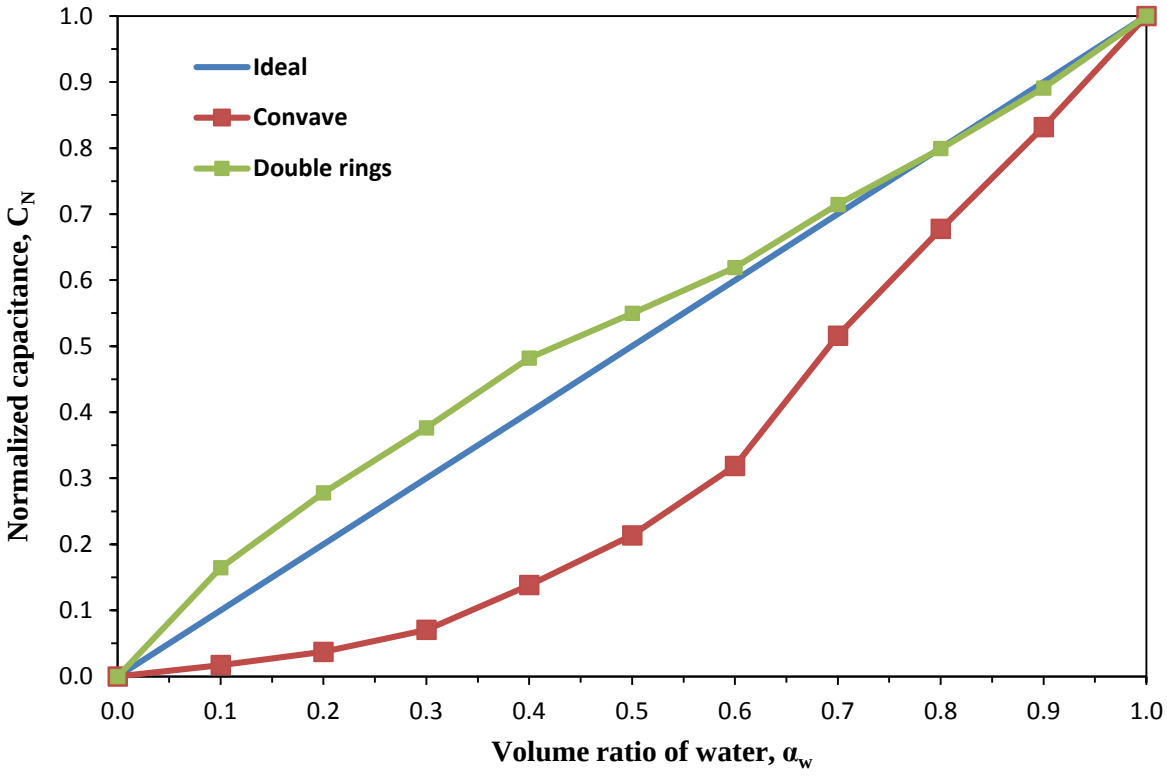

Figure 4.3: Comparison of linearity of response for concave and double rings electrodes

From Figure 4.3, it can be observed that for all volume ratios of water, concave electrodes tend to record capacitance values lower than the ideal values. Also, double rings electrodes tend to record the capacitance values higher than the ideal values.

Meanwhile, for every volume ratio of water, the absolute errors recorded from concave electrodes and double rings electrodes have been listed down in Table 4.6 below.

Table 4.6: Comparison of errors with respect to linearity of response

Volume ratio of water, α_w	Absolute error, E		ΔE = E (Concave) – E (double rings)
	Concave electrodes	Double rings electrodes	
0.10	0.08	0.06	0.02
0.20	0.16	0.08	0.08
0.30	0.23	0.08	0.15
0.40	0.26	0.08	0.18
0.50	0.29	0.05	0.24
0.60	0.28	0.02	0.26
0.70	0.18	0.01	0.17
0.80	0.12	0.00	0.12
0.90	0.07	0.01	0.06

From Table 4.6 above, it has been observed that for all volume ratios of water, α_w from 0.1 to 0.9, the absolute errors recorded by double rings electrodes are lower than that of double rings electrodes. It means that double rings electrodes are more accurate in measurement of capacitance values in pipelines with either low or high content of water.

In terms of mean absolute error, double rings electrodes are proven to be more superior with E= 0.043 or 4.3% compared to E= 0.186 or 18.6% for concave electrodes. Thus, if double rings electrodes are adopted over concave electrodes, the performance in terms of linearity of response will be higher with the advantage of smaller mean absolute error by $\Delta E = 0.186 - 0.043 = 0.143$ or 14.3%.

4.2 Sensitivity analysis on concave electrodes

The sensitivity of concave electrodes and double rings electrodes will be evaluated separately where the best design for each configuration will be identified. For both two-plate and four-plate models, the electric field distribution is shown in Figure 4.4 and Figure 4.5 respectively below, serving as the basis in this sensitivity analysis.

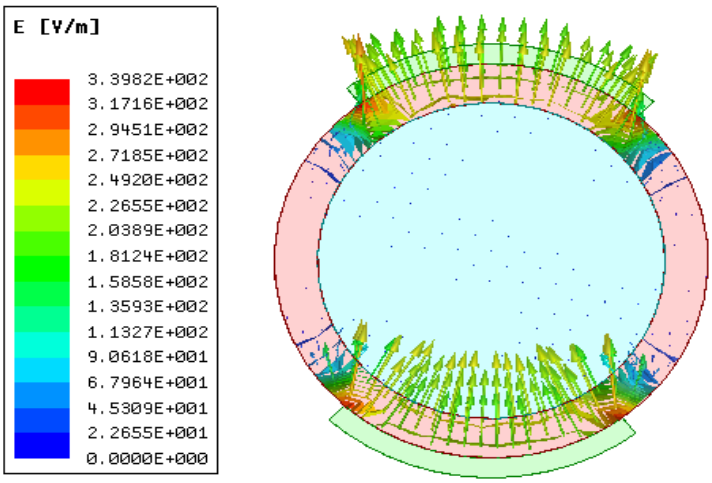

Figure 4.4: Electric field distribution of two-plate sensors (θ = 80˚)

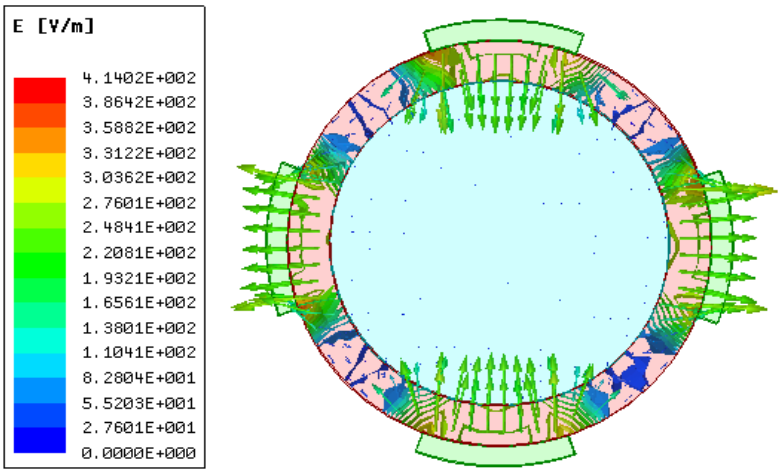

Figure 4.5: Electric field distribution of four-plate sensors (θ = 40˚)

In capacitance method, the electric field is created due to the potential difference between the electrodes which are assigned with different voltages. There is a similarity observed for two models displayed above, i.e. the electric field lines is flowing constantly in one direction from higher potential electrode (1V) towards the lower potential electrode (0V). For sensitivity analysis, capacitance measured depends on the location of elements distributed at all 246 parts of the fluid. Elements which fall within the electric field lines will result in higher capacitance. On the contrary, those which fall outside the electric field region will result in lower capacitance to be measured. Thus,

different angles of electrodes (θ) will produce different patterns of electric field distribution, resulting in different S_{avg} and SVP.

4.2.1 Two-plate capacitance sensors

The initial capacitance values for concave two-plate model (with fully filled oil and fully filled distilled water) with regards to different angles of electrodes are shown in Table 4.7 below. By utilizing the initial capacitance values, the results of sensitivity analysis in terms of S_{avg} and SVP are shown in Table 4.8 below. With that, the graphs of SVP and S_{avg} versus θ can be plotted for two-plate sensors as shown in Figure 4.6 below.

Table 4.7: Initial capacitance values for concave two-plate sensor

Angle of electrode, θ	**Capacitance at full distilled water, C (ε_h) (pF)**	**Capacitance at full oil, C (ε_l) (pF)**
60˚	0.22273	0.052167
70˚	0.25266	0.056702
80˚	0.28143	0.061404
90˚	0.31158	0.066448
100˚	0.34074	0.072235
110˚	0.36924	0.078641
120˚	0.40071	0.086181
130˚	0.43136	0.095384
40˚	0.46141	0.10669
150˚	0.49643	0.12209
160˚	0.53364	0.14481

Table 4.8: Results of sensitivity analysis for concave two-plate sensor

θ (˚)	**S_{avg}**	**SVP (%)**
60	1.0999	7.36
70	1.0577	6.45

80	1.0860	7.82
90	1.0350	5.30
100	1.1091	6.03
110	1.1892	7.35
120	1.1996	7.93
130	1.2869	9.91
140	1.4266	12.10
150	1.2743	16.14
160	1.4557	13.54

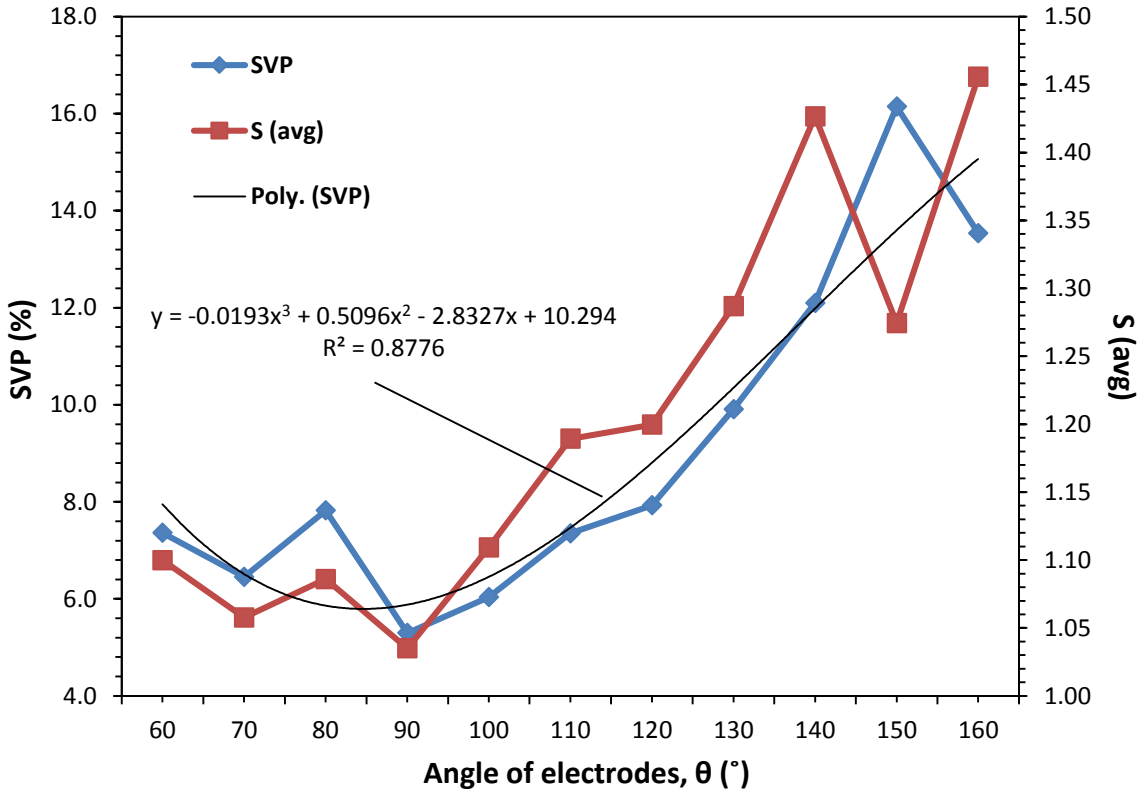

Figure 4.6: Effect of angles of electrodes on sensor sensitivity for two-plate sensors

Based on Figure 4.6 above, the S_{avg} values are relatively low and close to each other, ranging from 1.0350 to 1.4557. It means that the sensor relative sensitivity is generally low for all angles of electrodes using two-plate capacitance sensors. With respect to this, two-plate sensor with θ = 160˚ performs the best with the highest S_{avg} . Meanwhile, the

SVP values computed are relatively low, indicating a good homogeneity of sensitivity distribution. In terms of SVP, sensor with θ = 90˚ produces the best result with its SVP value of only 5.30%. In means that for θ = 90˚, the capacitance measurement results are proven to be least independent of the location of equal-volume elements.

In this case, the trend of SVP can be explained in three stages of electrodes angle as shown in Table 4.9 below. For better understanding, an illustration of the position of elements is provided in Figure 4.7 below. Also, it should be noted that the sensitivity analysis is governed by the basic equation in capacitance method as shown below:

$$C = \frac{\varepsilon * \varepsilon_a * A}{d}$$

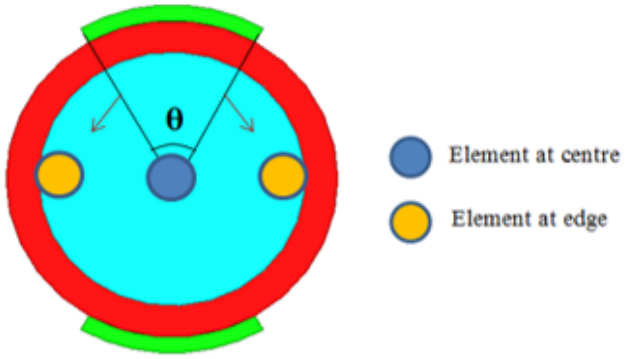

Figure 4.7: Position of elements with respect to change in electrodes angle

Table 4.9: Analysis on SVP for concave two-plate sensors

Stages	Analysis
60˚ < θ < 90˚	- Initially, SVP is high as the electric field is much stronger at the centre (higher capacitance measured) compared to the edge of the fluid. - When θ increases, SVP reduces as the coverage of electric field is expanding towards the edge of the fluid. - The difference in capacitance measured at the centre and edge is getting smaller.
θ = 90˚	- Here, SVP reaches minimum where the strength of electric field is equal across the fluid. - The homogeneity of capacitance measurement is maximum at

	this stage due to balanced electric field
90˚ < θ < 160˚	- When θ continues to increase, SVP increases as the electric field is increasingly stronger at the edge (higher capacitance measured) compared to the centre of the fluid. - The difference in capacitance measured at the centre and edge is getting larger.

4.2.1.1 Validation of results

There has been a previous research done by Zhao et al. in 2014 on liquid holdup measurement in horizontal oil–water two-phase flow using two-plate capacitance sensors [35]. Thus, the simulation results obtained here will be compared to the previous work as the benchmark to justify its credibility as shown in Figure 4.8 below.

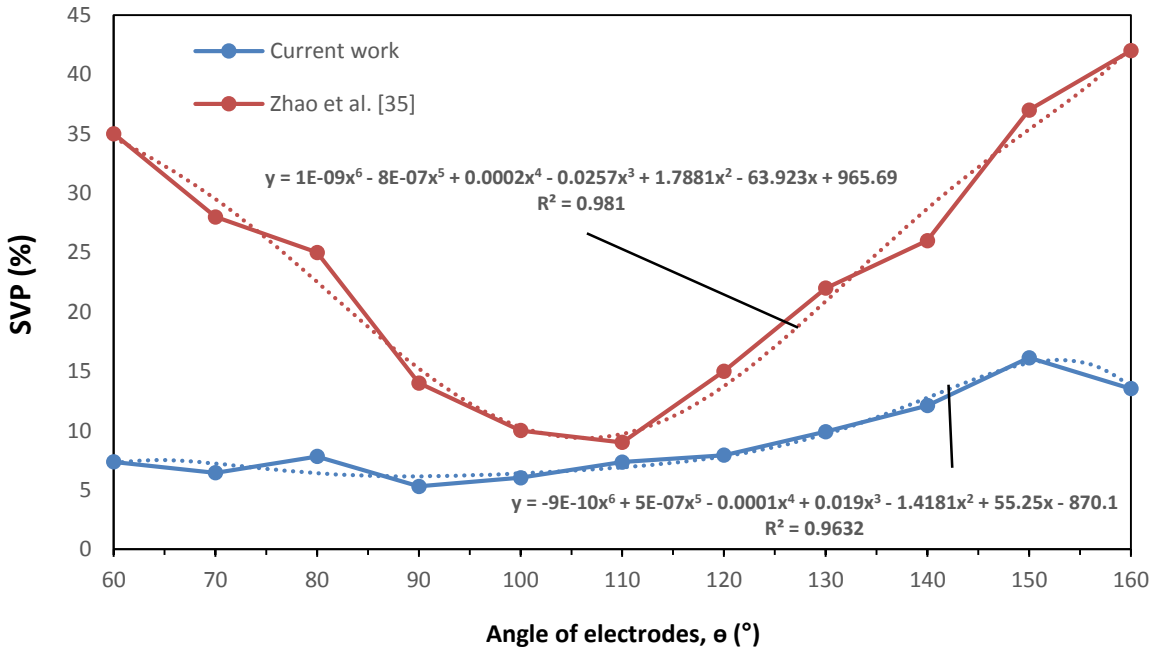

Figure 4.8: Comparison of SVP for two-plate sensors with previous work

Based on Figure 4.8 above, it can be observed that there is a similar trend observed in general in terms of the changes of SVP with angles of electrodes. In both cases, the SVP is initially high before it tends to drop until a minimum value which is determined to be 110° and 90° for previous work and current work respectively. After that point, the SVP for both cases rises again. With the similarity in trend with the previous work, the

current simulation results can be justified before moving on to the analysis on simulation results for four-plate capacitance sensors which will be described in the next section.

4.2.2 Four-plate capacitance sensors

The initial capacitance values for concave four-plate model (with fully filled oil and fully filled distilled water) with regards to different angles of electrodes are shown in Table 4.10 below. By utilizing the initial capacitance values, the results of sensitivity analysis in terms of S_{avg} and SVP are shown in Table 4.11 below. With that, the graphs of SVP and S_{avg} versus θ can be plotted in Figure 4.8 below.

Table 4.10: Initial capacitance values for concave four-plate sensor

Angle of electrodes, θ	**Capacitance at full distilled water, C (ε_h) (pF)**	**Capacitance at full oil, C (ε_l) (pF)**
30˚	0.2753	0.11738
35˚	0.30763	0.12728
40˚	0.34132	0.13827
45˚	0.37407	0.14923
50˚	0.4058	0.16223
55˚	0.4409	0.17739
60˚	0.47496	0.19428
65˚	0.51215	0.21552
70˚	0.55249	0.24125
75˚	0.59911	0.27536
80˚	0.65443	0.32397

Table 4.11: Results of sensitivity analysis for concave four-plate sensor

θ (˚)	**S_{avg}**	**SVP (%)**
30	3.3739	17.47
35	2.4829	18.75

40	3.9001	7.53
45	2.2755	26.70
50	3.8772	12.38
55	2.9889	8.44
60	2.9256	9.23
65	2.3616	21.32
70	4.2456	16.85
75	5.2807	51.57
80	2.9110	22.52

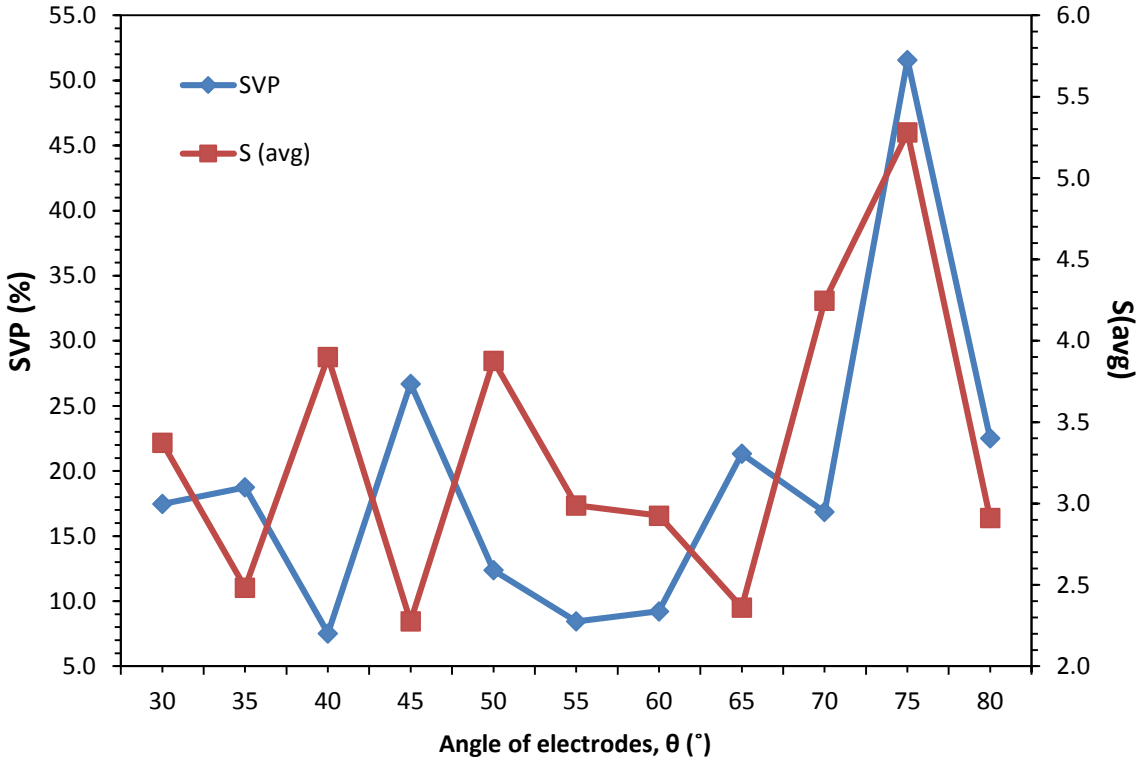

Figure 4.9: Effect of angles of electrodes on sensor sensitivity for four-plate sensors.

Based on Figure 4.9 above, the S_{avg} values are relatively high and of less consistency, ranging from 2.2755 to 5.2807. It means that the sensor relative sensitivity is generally high for all angles of electrodes using four-plate capacitance sensors. With respect to this, four-plate sensor with θ = 75˚ performs the best with the highest S_{avg}. Meanwhile,

the SVP values computed are relatively high, indicating a poor homogeneity of sensitivity distribution of four-plate capacitance sensors in general. In terms of SVP, sensor with $\theta = 40^{\circ}$ produces the best result with its SVP value of only 7.53%. In means that for $\theta = 40^{\circ}$, the capacitance measurement results are proven to be least independent of the location of equal-volume elements.

In this case, the trend of SVP is more difficult to be explained as compared to that of two-plate model. It should be noted that there has not been any research carried out on sensitivity analysis of concave four-plate capacitance sensors. Thus, validation of the result of sensitivity analysis for this model is not available at this moment.

4.2.3 Comparison of performance

After the sensitivity analysis on both two-plate and four-plate concave capacitance sensors has been performed with 11 different angles of electrodes (θ) for both designs, the comparison results are obtained and tabulated as shown in Table 4.12 below.

Table 4.12: Comparison of sensitivity results for two-plate and four-plate models

Two-plate sensors			**Four-plate sensors**		
θ (°)	**S_{avg}**	**SVP (%)**	**θ (°)**	**S_{avg}**	**SVP (%)**
60	1.0999	7.36	30	3.3739	17.47
70	1.0577	6.45	35	2.4829	18.75
80	1.0860	7.82	40	3.9001	7.53
90	1.0350	5.30	45	2.2755	26.70
100	1.1091	6.03	50	3.8772	12.38
110	1.1892	7.35	55	2.9889	8.44
120	1.1996	7.93	60	2.9256	9.23
130	1.2869	9.91	65	2.3616	21.32
140	1.4266	12.10	70	4.2456	16.85
150	1.2743	16.14	75	5.2807	51.57
160	1.4557	13.54	80	2.9110	22.52

For the comparison of sensitivity analysis on both two-plate sensors and four-plate sensors, it is found out that for all angles of electrodes, the four-plate sensors have advantage of higher sensitivity or detection ability of capacitance changes as compared to the two-plate sensors. However, for almost all equivalent angles of electrodes, the shift from two-plate design to four-plate design produces an undesirable result. This is because there is an increase in the SVP values, meaning the reduction in linearity of capacitance measurement results or the homogeneity of sensitivity distribution. Interestingly, there is an exception only for four-plate sensor with $\theta = 40^{\circ}$. At this electrodes angle, as compared to the two-plate sensor with $\theta = 80^{\circ}$, instead of rise, there is a drop in SVP values of 7.82 - 7.53 = 0.29 %. Also, S_{avg} is observed to be increased as well with an amount of 3.9001 - 1.0860 = 2.8141.

The increase in homogeneity of sensitivity at $\theta = 40^{\circ}$ for four-plate model is expected to be resulted from the optimum spacing between any two adjacent electrodes which is calculated as 50° with a total spacing of 200° on the model.

CHAPTER 5
CONCLUSION AND RECOMMENDATION

Capacitance method can be applied in oil and gas industry for the inspection of water content in crude oil in pipelines. By monitoring the concentration level of water, internal corrosion of pipeline walls can be minimized and it reduces the maintenance cost of oil and gas companies besides ensuring the safety of oil transportation.

At the end of this project, several conclusions have been obtained and the objectives have been met. Firstly, capacitance method is proven to be feasible to detect the presence of water in oil pipeline based on the simulation results using ANSYS Maxwell software. Also, for the detection of varied water content in oil-water mixture, double rings electrodes are better than concave electrodes in terms of linearity of response with lower mean absolute error of 14.3% recorded during the capacitance measurement.

Next, for the sensitivity analysis on concave electrodes, four-plate sensor is better than two-plate sensor in terms of sensor relative sensitivity (S_{avg}) for all angles of electrodes. For the sensitivity variation parameters (SVP), almost all angles of electrodes for four-plate sensors have lower linearity of capacitance measurement results. However, there is an exception for four-plate model with θ = 40˚ which is found out to be better than the two-plate model with θ = 80˚ in terms of SVP. This four-plate model configuration has an increase in S_{avg} of accompanied by the drop in SVP of 0.29 %. The increase in homogeneity of sensitivity distribution for four-plate model with θ = 40˚ can be investigated in future through further research.

For this project in general, there are several aspects that might affect the reliability of the outcome. For further improvement in terms of accuracy of results and continuity of this project, the recommendations are identified and listed down as follow:

i. The simulation can be done on flowing fluids instead of static fluids for better matching of real condition in oil transmission pipeline.

ii. Experimental works can be carried out in future to validate the simulation results in this paper especially for the comparison between two-plate capacitance sensors ($\theta = 80^{\circ}$) and four-plate capacitance sensors ($\theta = 40^{\circ}$).

These are the opportunities for further research to be carried out in the future to reduce the uncertainty in ANSYS Maxwell simulation results to enhance the existing capacitance method proposed in this project.

REFERENCES

[1] *Use of Pressure-Activated Sealant Technology to Cure Pipeline Leaks*, 2015. [Online]. Available: http://www.netl.doe.gov/research/oil-and-gas/project-summaries/completed-td/de-fc26-03nt41858. [Accessed: 24- Oct- 2015].

[2] P.Hopkins, *Underground Pipeline Corrosion*. Cambridge, UK: Woodhead Publishing Limited, 2014, pp. 62-84.

[3] J.Biomogi, S.Hernandez, J.Marin, E.Rodriguez, M.Lara and A.Viloria, Internal corrosion studies in hydrocarbons production pipelines located at Venezuelan Northeastern, *Chemical Engineering Research and Design*, vol. 90 (9), pp. 1159-1167, 2012.

[4] *Managing Corrosion of Pipelines that Transport Crude Oils*, 2013. [Online]. Available: http://www.pipelineandgasjournal.com/managing-corrosion-pipelines-transport-crude-oils?page=2 [Accessed: 24- Oct- 2015].

[5] R.Emerson and S.C.Diego, Experimental Study on Different Configurations of Capacitive Sensors for Measuring the Volumetric Concentration in Two-phase Flows, *Flow Measurement and Instrumentation*, vol. 37, pp. 127-134, 2014.

[6] D.M.G.Preethichandra and K.Shida, A Simple Interface Circuit to Measure Very Small Capacitance Changes in Capacitive Sensors, *IEEE Transactions on Instrumentation and Measurement*, vol. 50 (6), pp. 406-409, 2000.

[7] E.O. Maria, M.Juan and J.Genesca, CO2 corrosion control in steel pipelines. Influence of turbulent flow on the performance of corrosion inhibitors, *Journal of Loss Prevention in the Process Industries*, vol. 35, pp. 19-28, 2015.

[8] A.Jaworek and A.Krupa, Phase-shift detection for capacitance sensor measuring void fraction in two-phase flow, *Sensors and Actuators A: Physical*, vol. 160 (1-2), pp. 78-86, 2010.

[9] S.R.Wylie, A.Shaw and A.I.Al-Shamma'a, RF sensor for multiphase flow measurement through an oil pipeline, *Measurement Science and Technology*, vol. 17 (8), pp. 2141-2149, 2006.

[10] N.Ebbe and W.Arnstein, Measurement of Mixtures of Oil, Water, and Gas with Microwave Sensors. New Developments and Field Experience of the MFI MultiPhase, and WaterCut Meters of Roxar, *Subsurface Sensing Technologies and Applications II*, vol. 4129, pp. 12-21, 2000.

[11] V.M.Yu, A.P.Lifanov and A.S.Sovlukov, Microwave Measurement of Water Content in Flowing Crude Oil, *Automation and Remote Control*, vol. 74 (1), pp. 157-169, 2013.

[12] S.Lakar and S.Bordoloi, Monitoring of Moisture in Transformer Oil Using Optical Fiber as Sensor, *Journal of Photonics*, vol. 2013, 2013.

[13] C.C.Martijn, R.B.Victor, W.E.v.E.Carel, I.K.Zvonimir and M.S.Lex, X-Ray Spectrum Generation for a Multiphase Flow Meter, *IEEE Transactions on Nuclear Science*, vol. 50 (3), pp. 713-717, 2003.

[14] C.C.Martijn, R.B.Victor, W.E.v.E.Carel, I.K.Zvonimir and M.S.Lex ,The Optimal X-Ray Energy Problem in Multi-Phase Flow Metering, *IEEE Transactions on Nuclear Science*, vol. 50 (3), pp. 718-722, 2003.

[15] H.F.R.Mohd, A.R.Ruzairi, and A.R.Herlina, Gas Hold-Up Profiles Measurement Using Ultrasonic Sensor, *IEEE Sensors Journal*, vol. 11 (2), pp. 460-461, 2011.

[16] M. D. Silva, E. Schleicher, and U. Hampel. Capacitance Wire-mesh Sensor for Fast Measurement of Phase Fraction Distributions, *Measurement Science and Technology*, vol. 18 (7), pp. 2245, 2007.

[17] N.A.Tsochatzidis, T.D.Karapantsios, M.V.Kostoglou and A.J.Karabelast, A Conductance Probe for Measuring Liquid Fraction in Pipes and Packed, *International J.Multiphase Flow*, vol. 18 (5), pp. 653-667, 1992.

[18] S.Domenico, D,Marco, F.Vittorio and P.Pietro, Capacitance sensor for hold-up measurement in high-viscous-oil/conductive-water core-annular flows, *Flow Measurement and Instrumentation*, vol. 22 (5), pp. 360-369, 2011.

[19] T.Jarle and A.H.Erling, Capacitance sensor design for reducing errors in phase concentration measurements, *Flow Measurement and Instrumentation*, vol. 9 (1), pp. 25-32, 1998.

[20] H.Caniere, C.T'Joen, A.Willockx and M.D.Paeppe, Capacitance signal analysis of horizontal two-phase flow in a small diameter tube, *Experimental Thermal and Fluid Science*, vol. 32 (3), pp. 892-904, 2008.

[21] C.T.Chiang and Y.C.Huang, Semicylindrical Capacitive Sensor With Interface Circuit Used for Flow Rate Measurement, *IEEE Sensors Journal*, vol. 6 (6), pp. 1564-1570, 2006.

[22] C.Tan, P.Li, W.Dai and F.Dong, Characterization of oil–water two-phase pipe flow with a combined conductivity/ capacitance sensor and wavelet analysis, *Chemical Engineering Science*, vol. 134, pp.153-168, 2015.

[23] S.I.I.Ahmad, I.Issham, Z.Mansoor, M.Rahmat, P.Ali, S.M.Mohd and Z.S.Mior, Review of oil–water through pipes, *Flow Measurement and Instrumentation*, vol. 45, pp. 357-374, 2015.

[24] P.Angeli and G.F.Hewitt, Flow structure in horizontal oil-water flow, *International Journal of Multiphase Flow*, vol. 26 (7), pp. 1117-1140, 2000.

[25] B.D.Anand, K.D.Ashok and K.M.Tapas, An appraisal of viscous oil–water two-phase flow through an undulated pipeline in peak configuration, *Experimental Thermal and Fluid Science*, vol. 68, pp. 177-186, 2015.

[26] A.Maher and Z.A.Muhammad, An Interface Circuit Design Based On Differential Capacitive Sensors for Accurate Measurement of Water Contents in Crude Oil, *Conference: Circuits and Systems (ICCAS)*, pp. 263-266, 2012.

[27] J.Ye, L.Peng, W.Wang and W.Zhou, Helical Capacitance Sensor-Based Gas Fraction Measurement of Gas–Liquid Two-Phase Flow in Vertical Tube with Small Diameter, *IEEE Sensors Journal*, vol. 11 (8), pp. 1704-1710, 2011.

[28] L.Zhai, N.Jin, Z.Gao and Z.Wang, Liquid holdup measurement with double helix capacitance sensor in horizontal oil–water two-phase flow pipes, *Chinese Journal of Chemical Engineering*, vol. 23 (1), pp. 268-275, 2015.

[29] M.S.A. Abouelwafa, E.J.M. Kendall, The use of capacitance sensors for phase percentage determination in multiphase pipelines, *IEEE Trans. Instrum. Meas.*, vol. 29 (1), pp. 24-27, 1980.

[30] J.J.M. Geraets, J.C. Borst, A capacitance sensor for two-phase void fraction measurement and flow pattern identification, *Int. J.Multiphase Flow*, vol. 14 (3), pp. 305–320, 1988.

[31] E.A. Hammer, J. Tollefsen, K. Olsvik, Capacitance transducers for nonintrusive measurement of water in crude oil, *Flow Meas. Instrum*., vol. 10, pp. 262–268, 1989.

[32] C.G. Xie, A.L. Stott, A. Plaskowski, M.S. Beck, Design of capacitance electrodes for concentration measurements of two-phase flow, *Meas. Sci. Technol.*, vol. 1, pp. 65–78, 1990.

[33] H. Caniere, C. T'Joen, Horizontal two-phase flow characterization for small diameter tubes with a capacitance sensor, *Meas. Sci. Technol.*, vol. 18, pp. 2898–2906, 2007.

[34] K. De Kerpel, B. Ameel, C. T'Joen, H. Caniere, M. De Paepe, Flow regime based calibration of a capacitive void fraction sensor for small diameter tubes, *Int. J. Refrig*., vol. 36, pp. 390–401, 2013.

[35] A.Zhao, N.Jin, L.Zhai and Z.Gao, Liquid holdup measurement in horizontal oil–water two-phase flow by using concave capacitance sensor, *Measurement*, vol. 49, pp. 153-163, 2014.

APPENDICES

Table A1: List of dielectric constant for common fluids

Table A2: Sample data for sensitivity analysis on concave two-plate model ($\theta = 80^{\circ}$)

Table A3: Sample data for sensitivity analysis on concave four-plate model ($\theta = 40^{\circ}$)

Table A1: List of dielectric constant for common fluids

Fluid	**Dielectric constant, Ɛ**
Acetic Acid	6.2
Acetone	20.7
Alcohol, ethyl (ethanol)	24.3
Benzene	2.3
Bromine	3.1
Butane	1.4
Carbon tetrachloride	2.23
Castor Oil	4.7
Chlorine	2.0
Ether	4.3
Ethylamine	6.3
Gasoline	2.0
Glycerol	42.5
Hexane	2.0
Kerosene	1.8
Naphthalene	2.5
Oxygen	1.51
Palmitic Acid	2.3
Pentane	1.8
Propane	1.6
Stearic Acid	2.3
Styrene	2.4
Water	80.4

Table A2: Sample data for sensitivity analysis on concave two-plate model ($\theta = 80^{\circ}$)

Element, i	C_w (pF)	C_o(pF)	C_i (pF)	V_T (mm^3)	V_i (mm^3)	S_i	S_{avg}	$(S_i - S_{avg})^2$
1	0.28143	0.061404	0.06229	604.6947	2.356194	1.033438971	1.086022236	0.002765
2	0.28143	0.061404	0.06228	604.6947	2.356194	1.021774874	1.086022236	0.004127724
3	0.28143	0.061404	0.06237	604.6947	2.356194	1.126751745	1.086022236	0.001658893
4	0.28143	0.061404	0.06234	604.6947	2.356194	1.091759455	1.086022236	3.29157E-05
5	0.28143	0.061404	0.06238	604.6947	2.356194	1.138415842	1.086022236	0.00274509
6	0.28143	0.061404	0.06242	604.6947	2.356194	1.185072229	1.086022236	0.009810901
7	0.28143	0.061404	0.06238	604.6947	2.356194	1.138415842	1.086022236	0.00274509
8	0.28143	0.061404	0.06242	604.6947	2.356194	1.185072229	1.086022236	0.009810901
9	0.28143	0.061404	0.06245	604.6947	2.356194	1.220064519	1.086022236	0.017967333
10	0.28143	0.061404	0.06245	604.6947	2.356194	1.220064519	1.086022236	0.017967333
11	0.28143	0.061404	0.06242	604.6947	2.356194	1.185072229	1.086022236	0.009810901
12	0.28143	0.061404	0.06225	604.6947	2.356194	0.986782584	1.086022236	0.009848509
13	0.28143	0.061404	0.06233	604.6947	2.356194	1.080095358	1.086022236	3.51279E-05
14	0.28143	0.061404	0.06239	604.6947	2.356194	1.150079938	1.086022236	0.004103389
15	0.28143	0.061404	0.06231	604.6947	2.356194	1.056767165	1.086022236	0.000855859
16	0.28143	0.061404	0.06223	604.6947	2.356194	0.963454391	1.086022236	0.015022877
17	0.28143	0.061404	0.06222	604.6947	2.356194	0.951790294	1.086022236	0.018018214
18	0.28143	0.061404	0.06219	604.6947	2.356194	0.916798004	1.086022236	0.028636841
19	0.28143	0.061404	0.06233	604.6947	2.356194	1.080095358	1.086022236	3.51279E-05
20	0.28143	0.061404	0.06229	604.6947	2.356194	1.033438971	1.086022236	0.002765
21	0.28143	0.061404	0.0623	604.6947	2.356194	1.045103068	1.086022236	0.001674378
22	0.28143	0.061404	0.06225	604.6947	2.356194	0.986782584	1.086022236	0.009848509
23	0.28143	0.061404	0.06226	604.6947	2.356194	0.998446681	1.086022236	0.007669478
24	0.28143	0.061404	0.0623	604.6947	2.356194	1.045103068	1.086022236	0.001674378

Table A3: Sample data for sensitivity analysis on concave four-plate model ($\theta = 40^{\circ}$)

Element, i	C_w (pF)	C_o(pF)	C_i (pF)	V_T (mm^3)	V_i (mm^3)	S_i	S_{avg}	$(S_i - S_{avg})^2$
1	0.34132	0.13827	0.1412	604.6947	2.356194	3.703307229	3.900089419	0.03872323
2	0.34132	0.13827	0.1415	604.6947	2.356194	4.082485444	3.900089419	0.03326831
3	0.34132	0.13827	0.1415	604.6947	2.356194	4.082485444	3.900089419	0.03326831
4	0.34132	0.13827	0.141	604.6947	2.356194	3.450521753	3.900089419	0.202111087
5	0.34132	0.13827	0.1413	604.6947	2.356194	3.829699967	3.900089419	0.004954675
6	0.34132	0.13827	0.1412	604.6947	2.356194	3.703307229	3.900089419	0.03872323
7	0.34132	0.13827	0.141	604.6947	2.356194	3.450521753	3.900089419	0.202111087
8	0.34132	0.13827	0.1412	604.6947	2.356194	3.703307229	3.900089419	0.03872323
9	0.34132	0.13827	0.1408	604.6947	2.356194	3.197736276	3.900089419	0.493299937
10	0.34132	0.13827	0.1409	604.6947	2.356194	3.324129015	3.900089419	0.331730388
11	0.34132	0.13827	0.1412	604.6947	2.356194	3.703307229	3.900089419	0.03872323
12	0.34132	0.13827	0.1412	604.6947	2.356194	3.703307229	3.900089419	0.03872323
13	0.34132	0.13827	0.1411	604.6947	2.356194	3.576914491	3.900089419	0.104442034
14	0.34132	0.13827	0.1414	604.6947	2.356194	3.956092705	3.900089419	0.003136368
15	0.34132	0.13827	0.1414	604.6947	2.356194	3.956092705	3.900089419	0.003136368
16	0.34132	0.13827	0.141	604.6947	2.356194	3.450521753	3.900089419	0.202111087
17	0.34132	0.13827	0.1412	604.6947	2.356194	3.703307229	3.900089419	0.03872323
18	0.34132	0.13827	0.1415	604.6947	2.356194	4.082485444	3.900089419	0.03326831
19	0.34132	0.13827	0.1415	604.6947	2.356194	4.082485444	3.900089419	0.03326831
20	0.34132	0.13827	0.1412	604.6947	2.356194	3.703307229	3.900089419	0.03872323
21	0.34132	0.13827	0.141	604.6947	2.356194	3.450521753	3.900089419	0.202111087
22	0.34132	0.13827	0.1411	604.6947	2.356194	3.576914491	3.900089419	0.104442034
23	0.34132	0.13827	0.1411	604.6947	2.356194	3.576914491	3.900089419	0.104442034
24	0.34132	0.13827	0.1411	604.6947	2.356194	3.576914491	3.900089419	0.104442034